Check for updates

Transactions in GIS

WILEY

Transactions in GIS

RESEARCH ARTICLE

High-Accuracy Flood Susceptibility Mapping and Risk Assessment in a Touristic Sub-Basin: Utilizing Analytic Hierarchy Process With the Most Effective Factors

İbrahim Arslan[1] | Serdar Selim[2]

[1]Remote Sensing and Geographic Information Systems Graduate Program, Institute of Natural and Applied Sciences, Akdeniz University, Antalya, Turkey | [2]Department of Space Sciences and Technologies, Faculty of Science, Akdeniz University, Antalya, Turkey

Correspondence: Serdar Selim (serdarselim@akdeniz.edu.tr)

Received: 10 May 2025 | **Revised:** 31 December 2025 | **Accepted:** 7 January 2026

Keywords: Alanya (Dim River) sub-basin | data-scarce regions | flood management | multi-criteria decision analysis | remote sensing and geographic information system

ABSTRACT

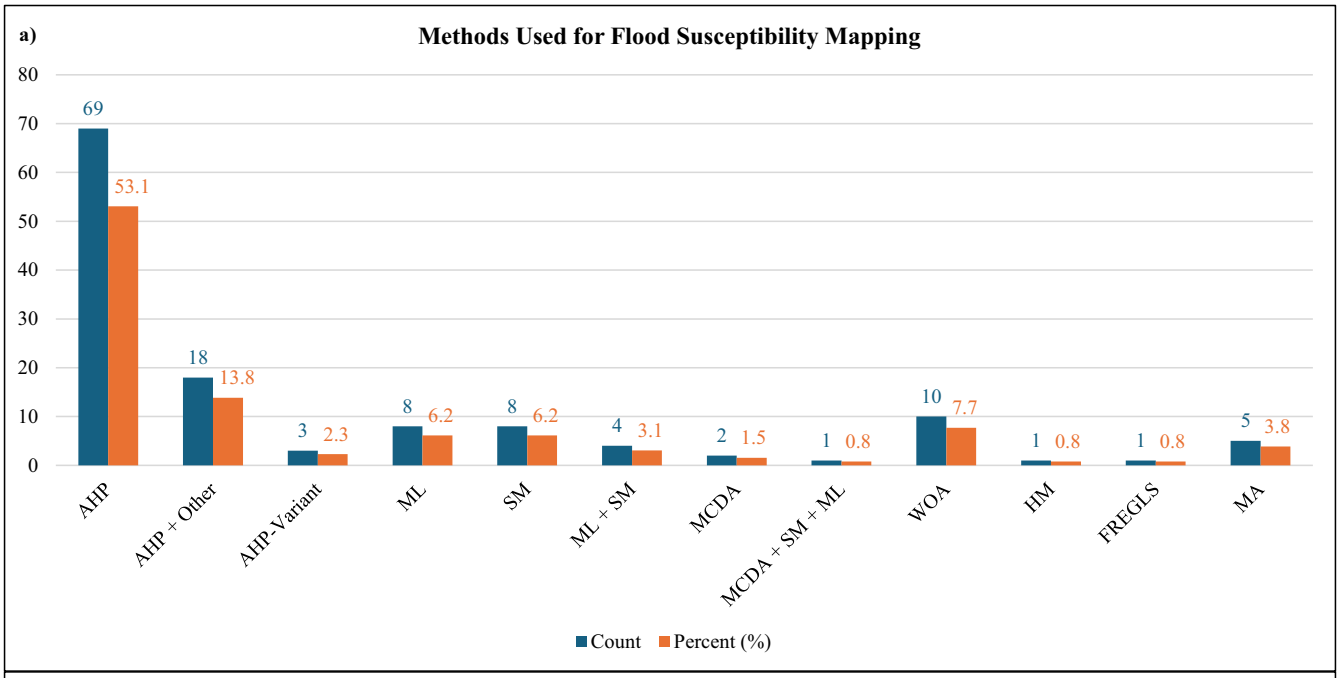
This study aimed to map flood susceptible areas and assess potential impacts at the sub-basin scale in a densely populated touristic region. For this purpose, seven flood conditioning factors were selected: slope, land use/land cover, elevation, rainfall, distance from river, soil, and drainage density. Geographic information system-based analytic hierarchy process (AHP) was used to map flood susceptibility. To validate the flood susceptibility map, a flood inventory map derived from satellite-based remotely sensed imagery (both optical and synthetic aperture radar) was used, and the validation showed a high accuracy of 93.2%. It was found that urban and agricultural areas are the most susceptible to flooding, and most of the hotels and historical/tourist attractions in the region are at risk. The findings highlight that AHP with widely used factors yields reliable results even in data-scarce regions. This approach can assist decision-makers in developing appropriate flood risk management strategies.

1 | Introduction

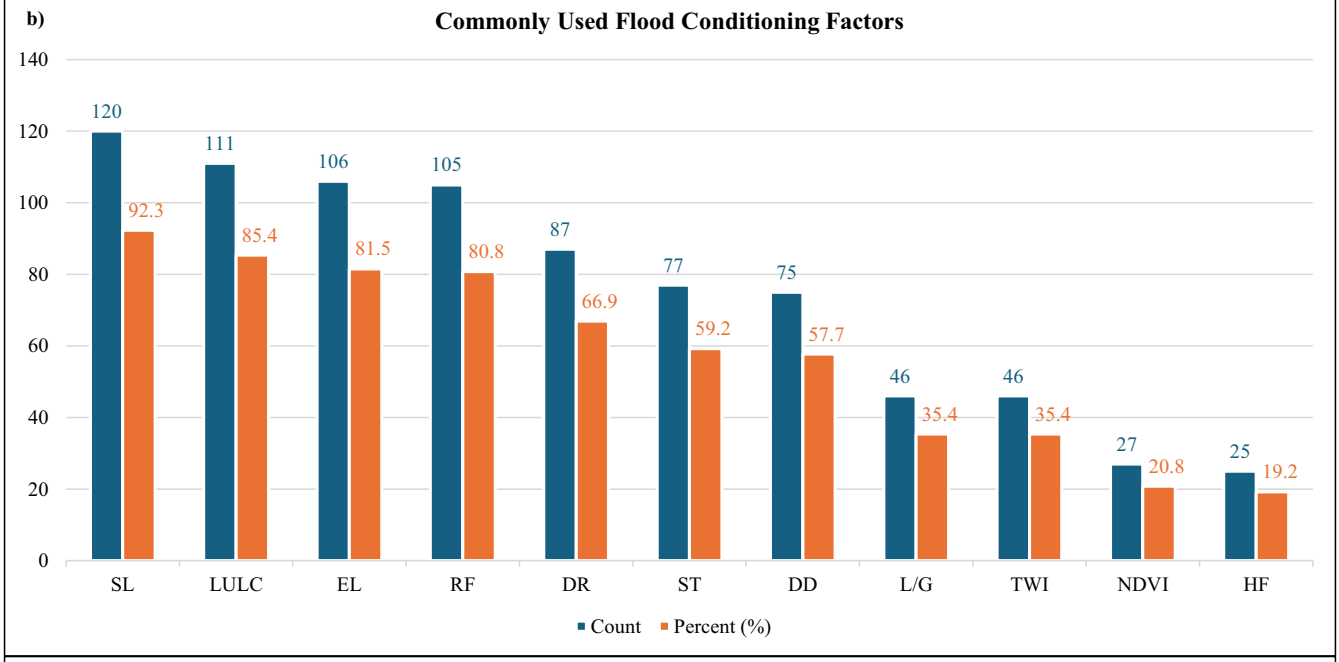
Floods are one of the most destructive hazards that occur frequently around the world (Akdeniz and Tuzcu 2023; Baykal et al. 2023), causing loss of life and property, and severe damage to infrastructure (Belazreg et al. 2024; Chaulagain et al. 2023; Ghosh et al. 2023; Vafa and Seker 2023). Moreover, floods can destroy crops that provide food for people and animals, leading to significant economic losses (Bhuyan et al. 2024), furthermore, they disrupt transportation and trigger other natural disasters such as landslides (Isiaka et al. 2023). Since flood-related damage and deaths are predicted to increase in the future with the increase in sudden and excessive rainfall as a result of global climate change (Aydin and Sevgi Birincioğlu 2022; Belazreg et al. 2024; Gautam and Singh 2022), it is important to identify flood-prone areas in order to prevent or minimize the impact of floods (Enomah et al. 2023; Gahalod et al. 2024; Nadège et al. 2023; Selvam and Antony Jebamalai 2023).

There are many recent studies in the literature on flood susceptibility mapping and risk assessment in order to prevent or minimize the possible destructive effects of floods. In these studies: (i) expert knowledge based methods (such as AHP), (ii) statistical methods (such as frequency ratio (FR)), (iii) machine learning (ML) methods (such as artificial neural network (ANN)), (iv) hydrological models (such as Hydrologic Engineering Center River Analysis System (HEC-RAS)), (v) weighted overlay analysis, and (vi) morphometric analysis have been used. Figure 1 and Appendix A (Table A1) show the results of the most recent literature review on flood susceptibility mapping and flood risk assessment published in the last 5 years, between 2019 and the first quarter of 2024. The

© 2026 John Wiley & Sons Ltd.



Abbreviations: *AHP:* Analytic Hierarchy Process; *ML:* Machine Learning Techniques; *SM:* Statistical Methods; *MCDA:* Multi-Criteria Decision Analysis (other than AHP); *WOA:* Weighted Overlay Analysis; *HM:* Hydrological Methods; *FREGLS:* It takes its name from the initials of the factors taken into account (Kourgialas and Karatzas 2016); *MA:* Morphological Analysis



Abbreviations: *SL:* Slope; *LULC:* Land Use/Land Cover; *EL:* Elevation; *RF:* Rainfall; *DR:* Distance from River; *ST:* Soil Type/Texture; *DD:* Drainage Density; *L/G:* Lithology/Geology; *TWI:* Topographic Wetness Index; *NDVI:* Normalized Difference Vegetation Index; *HF:* Historical Floods

FIGURE 1 | (a) Methods used and (b) factors considered in flood susceptibility mapping and risk assessment (literature review between 2019 and the first quarter of 2024).

literature review was performed via Google Scholar using the primary keywords "flood risk assessment" and "flood susceptibility mapping." The primary criteria for including a paper in this review (130 in total) were the explicit documentation of the methodologies, the clear definition of flood conditioning factors, and that the publication was in English. As shown in Figure 1a and Appendix A (Table A1), it can be said that AHP is the most frequently used method for flood susceptibility mapping and risk assessment (Nsangou et al. 2022).

Previous studies have observed that the AHP method achieves results of high accuracy (Ahmed et al. 2024; Gahalod et al. 2024; Ghosh et al. 2023; Khan and Jhamnani 2024; Nsangou et al. 2022), with some studies emphasizing the superiority of

14679671, 2026, 1, Downloaded from https://onlinelibrary.wiley.com/doi/10.1111/tgis.70190 by Serdar Selim - Akdeniz University , Wiley Online Library on [08/02/2026]. See the Terms and Conditions (https://onlinelibrary.wiley.com/terms-and-conditions) on Wiley Online Library for rules of use; OA articles are governed by the applicable Creative Commons License

this method in comparison with other methods (Cabrera and Lee 2019; Chen 2022). Geographic information system (GIS) has historically been well used to accurately determine potential risk zones for natural disasters (Baykal et al. 2023; Nadège et al. 2023). The GIS-based AHP method has been reported as a reliable and useful tool for risk assessment in areas with data scarcity due to its flexibility, ease of use, cost, and time effectiveness; where it can be applied anywhere in the world (Alimi et al. 2023; Bansal et al. 2023; Dash and Sar 2020; Mitra et al. 2022; Purwanto et al. 2022).

There are also hydrological modeling approaches (Louis et al. 2024; Sarchani et al. 2020), ranging from simple one-dimensional (Pathan and Agnihotri 2021) to complex two- or three-dimensional models (Luo et al. 2022; Sebastian et al. 2022) for predicting flood depth and velocity (Louis et al. 2024; Sarchani et al. 2020; Kaya and Üneş 2025; Selim et al. 2024) through specialized software such as HEC-RAS, FLO-2D, SRH-2D, IBER, MIKE SHE, TUFLOW, River-Flow2D, and LISFLOOD-FP (Iroume et al. 2022; Trif et al. 2023). However, their implementation is often constrained. The AHP method is particularly advantageous, especially in developing countries such as Turkey, where the lack of spatial data on historical flood events renders statistical or machine learning methods inapplicable. Consequently, AHP-based flood susceptibility mapping remains highly relevant, as it utilizes open-access data, offers multi-criteria decision-making capabilities, and provides efficient results without requiring specialized modeling expertise.

In addition to the method used, the selection of flood conditioning factors is of great importance. In fact, this process is one of the most important steps to produce reliable and highly accurate flood susceptibility maps (Vajeethaveesin et al. 2022). A large number of factors with different weights have been used in AHP-based flood susceptibility mapping and flood risk assessment studies. It is known that these factors can vary and depend on the characteristics of the study area (physical, climatic, economic). However, it is expected that the inclusion of different factors with different weights in the AHP process may affect the accuracy and cause researchers to waste time on which factors should be used. For this reason, in order to get the right results quickly and practically in flood susceptibility mapping and flood risk assessment studies, the most frequently used factors in the articles published in the literature in the last 5 years have been identified and are shown in Figure 1b and Appendix A (Table A1).

After earthquakes, floods are the second most frequent natural disaster in Turkey, causing the greatest loss of life and property (Gurer and Ozguler 2004). In a review by Haltas et al. (2021), it was found that a total of 2101 flood events occurred in Turkey during a 90-year period, between 1930 and 2020; and that the impact of flooding increased exponentially during this period due to an increase in population and urbanization. It was found that 1 in 10 floods in Turkey resulted in loss of life, and the average loss of life per flood for this period's floods was 4.98 (Haltas et al. 2021). Historically, the most significant flood events were reported in the Black Sea and Mediterranean Regions, due to heavy rainfall. In a study conducted by Koç and Thieken (2018), it was observed that Antalya, located in the Mediterranean Region, ranked second out of 55 flood events over a 60-year period, between 1960 and 2014.

As a direct result of the floods, studies have been conducted to identify flood-prone areas in the Mediterranean Region. Özdemir et al. (2023) focused their study on the Eastern Mediterranean Basin, located in the eastern part of the Mediterranean Region. Baykal et al. (2023) applied the AHP method in the Küçük Aksu River Basin, another sub-basin of the Antalya Basin. However, there is no study on flood susceptibility mapping and risk assessment in the densely populated Alanya Sub-Basin (also known as the Dim River Sub-Basin of the Antalya Basin), which hosts important historical and tourist attractions of the region. The fact that the region has a dense population and tourist concentration, especially in the coastal areas, means a possible flood disaster can significantly affect these regions, which emphasizes the importance of a study to be conducted in this region. It is predicted that in the event of a possible flood disaster, the tourism sector, which is the main source of livelihood of the region, would be directly affected and likely suffer considerable economic losses. In order to prepare flood disaster risk management plans in advance, it is of great importance to analyze the flood risk by mapping flood susceptible areas at the sub-basin scale, enabling mitigation to minimize the flood impact. Such a study to be conducted in the region will be the first study in the literature to assess the potential flood risk associated with tourist facilities and has the potential to ensure that the region can strategically prepare for a possible disaster by identifying the flood susceptibility of these facilities.

The main objective of this study is to map the flood susceptible areas and assess the potential impacts in the Alanya Sub-Basin of Antalya Basin, Turkey. The flood conditioning factors were selected by considering the most frequently used factors in the literature: slope, land use/land cover (LULC), elevation, rainfall, distance from river, soil, and drainage density. The GIS-based AHP method, which is the most frequently used method in the literature, was used for flood susceptibility mapping. Considering the weights of the factors determined by AHP, the weighted overlay was performed in the GIS environment, and the flood-prone areas in the region were mapped. This analysis enables a comprehensive discussion of the potential impacts and consequences associated with flood disasters in the region. To ensure reliability, the accuracy of the resulting flood susceptibility map is validated using a flood inventory map derived from a combination of synthetic aperture radar (SAR) and multispectral satellite imagery. To the best of our knowledge, this study represents the first instance in the literature where SAR and multispectral datasets are integrated specifically to evaluate the accuracy of a flood susceptibility map.

2 | Materials and Methods

2.1 | Study Area

This study was conducted in the Alanya Sub-Basin, also known as the Dim River Sub-Basin of the Antalya Basin, Turkey. This sub-basin is located between latitudes 36°23′29.66″ N and 37°02′11.10″ N and longitudes 31°27′52.14″ E and 32°23′21.11″ E (Figure 2). The total area of the sub-basin is 2988.59 km^2. According to the LULC map created by classifying CORINE Land Cover (2018) data, there are four main land covers: urban areas (46.43 km^2 (1.6%)), agricultural areas

14679671, 2026, 1, Downloaded from https://onlinelibrary.wiley.com/doi/10.1111/tgis.70190 by Serdar Selim - Akdeniz University , Wiley Online Library on [08/02/2026]. See the Terms and Conditions (https://onlinelibrary.wiley.com/terms-and-conditions) on Wiley Online Library for rules of use; OA articles are governed by the applicable Creative Commons License

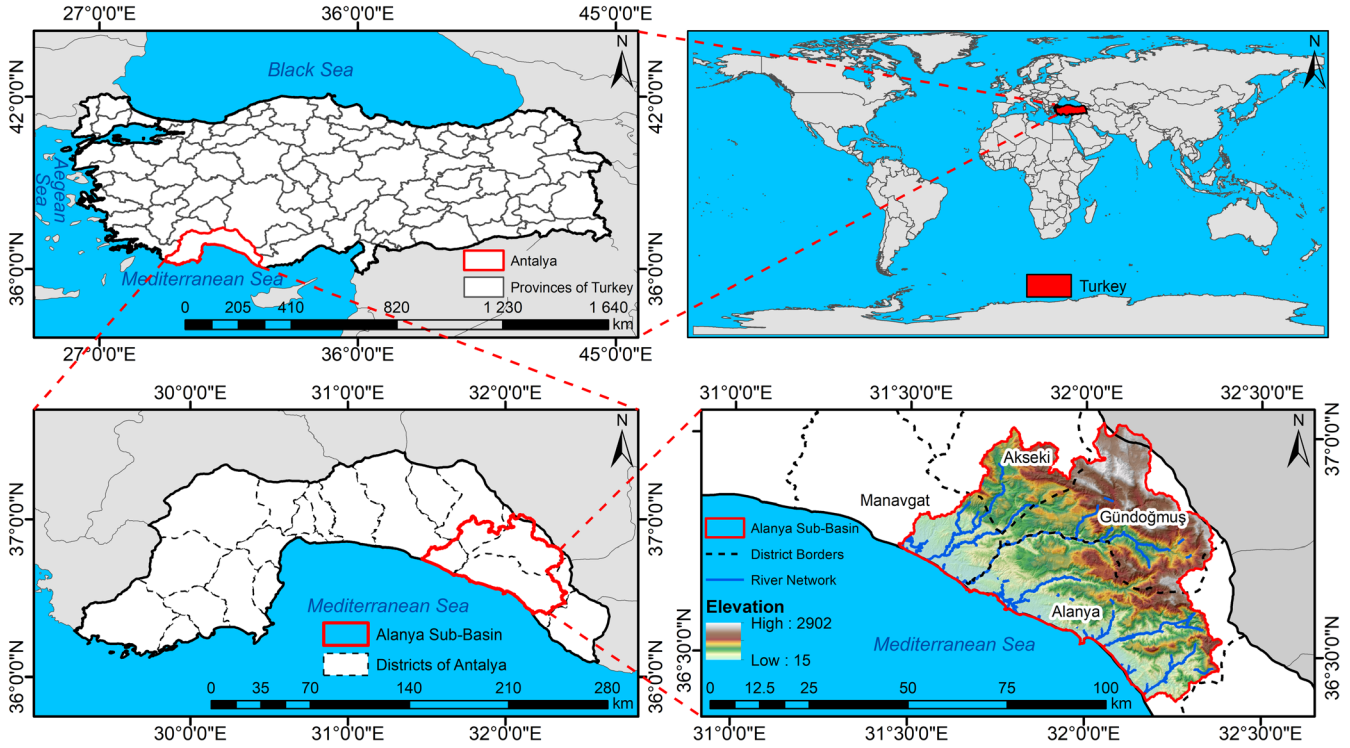


FIGURE 2 | Location map of the study area.

(658.31 km^2 (22.0%)), forested areas (2273.64 km^2 (76.1%)), and water bodies (10.21 km^2 (0.3%)). The altitude varies between 15 and 2902 m. There are different major soil groups in the region, such as alluvial soils, colluvial soils, hydromorphic soils, red and red-brown Mediterranean soils, brown and non-limestone brown forest soils, high mountain meadow soils, regosols, and rendzinas. Active rivers include the Dim River, Oba River, Kargı River, Karpuz River, and Alara (Ulugüney) River in the sub-basin. These rivers flow out to the Mediterranean Sea, passing through a low elevation, shallow sloped, densely populated coastal area.

The sub-basin is dominated by a Mediterranean climate. Summers are hot and dry, while winters are mild and moderately rainy. According to the meteorological measurements made by the Turkish State Meteorological Service (TSMS) (TSMS 2024) between 1930 and 2023, the lowest average temperature in the region was 10.0°C in January, the highest average temperature 28.6°C in July and the annual average temperature 18.8°C. July has the fewest rainy days with an average of 0.53 days per month, while January has the highest with an average of 12.5 rainy days per month. The annual total number of days it rained was 73.5 days. The lowest total rainfall is 4.3 mm in August, the highest total rainfall is 256.1 mm in December, and the total annual rainfall 1053.4 mm (TSMS 2024).

The sub-basin is densely populated. According to the 2023 population data of the Turkish Statistical Institute (TURKSTAT) (TURKSTAT 2024), the sub-basin population of the districts of Alanya, Manavgat, Akseki and Gündoğmuş is 359,891, 258,367, 11,896, and 8259 people, respectively, with a total population of 638,413. Although the sub-basin does not completely cover the borders of these districts, considering that the population is concentrated in the coastal areas, it can be said that approximately one in four of the total population of Antalya (2,696,249) lives in this region. In addition to its beautiful climate and geography, the sub-basin also hosts important historical castles and ancient cities, as well as tourist attractions, such as caves, beaches, natural beauty spots, and entertainment venues. These features drive the intensity in tourists in this area. According to the 2023 tourism data of the Ministry of Culture and Tourism (MCT) (MCT 2024), the number of foreign tourists that visited certified accommodation facilities in the districts of the sub-basin in 2023 is 6,076,796, 6,363,286, 47, and 1553 people for Alanya, Manavgat, Akseki, and Gündoğmuş, respectively. Together with domestic tourists, these numbers reach 7,093,599, 7,112,462, 1434, and 21,963 people, respectively, with a total population of 14,229,458. Therefore, the population of the sub-basin increases significantly with the domestic and foreign tourists coming to the region, especially in the summer season.

2.2 | Datasets and Data Preparation

Information on the data used and their characteristics is summarized in Table 1. All data used in the study were provided free of charge.

2.2.1 | Flood Conditioning Factors

The selection of flood conditioning factors has a significant impact on the accuracy of flood susceptibility mapping. However, since there is no universal consensus on how to select these factors (Msabi and Makonyo 2021), the appropriate selection is a challenge (M Amen et al. 2023). In this study, flood conditioning factors were selected using a literature review. A total of 130

14679671, 2026, 1, Downloaded from https://onlinelibrary.wiley.com/doi/10.1111/tgis.70190 by Serdar Selim - Akdeniz University , Wiley Online Library on [08/02/2026]. See the Terms and Conditions (https://onlinelibrary.wiley.com/terms-and-conditions) on Wiley Online Library for rules of use; OA articles are governed by the applicable Creative Commons License

TABLE 1 | Data used and their characteristics.

	Purpose	Data	Data description	Data source	Data format	Data resolution/ Scale
Flood susceptibility mapping	Elevation, slope	DEM	ALOS PALSAR DEM	Alaska Satellite Facility (ASF) Data Search Vertex (https://search.asf.alaska.edu/#/)	Raster	12.5 m
	Level 1 LULC	LULC	CORINE Land Cover (2018)	Copernicus Land Monitoring Service (https://land.copernicus.eu/en/map-viewer)	Vector	—
	Distance from river, drainage density	River	Active river network	Open Street Map (OSM) (https://www.openstreetmap.org/export#)	Vector	—
	Average annual rainfall	Rainfall	Monthly rainfall amounts measured by 8 different meteorological stations	Akdeniz University, Remote Sensing and Geographic Information Systems Graduate Program Database	Vector	—
	Soil permeability	Soil	Major soil group type and soil characteristics	Akdeniz University, Remote Sensing and Geographic Information Systems Graduate Program Database	Vector	1:25.000
Socioeconomic factors exposed to flooding	Population density	Population	Address based population registration system results: Population of municipalities, villages and quarters (2023)	Turkish Statistical Institute (TURKSTAT) (https://biruni.tuik.gov.tr/medas/?locale=en)	Excel	—
		Settlement	Point-based settlement areas	Open Street Map (OSM) (https://www.openstreetmap.org/export#)	Vector	—
	Farmlands	Soil	Land capability classes	Akdeniz University, Remote Sensing and Geographic Information Systems Graduate Program Database	Vector	—
	Road network	Road	Major road network	Open Street Map (OSM) (https://www.openstreetmap.org/export#)	Vector	—
	Historical and touristic attractions	Historical/ touristic place	Historical and touristic places such as ancient cities, historical castles, caves, etc.	Open Street Map (OSM) (https://www.openstreetmap.org/export#)	Vector	—
	Hotel locations	Hotel	Hotel locations where tourists stay	Open Street Map (OSM) (https://www.openstreetmap.org/export#)	Vector	—
Validation	Flood inventory mapping	Satellite-based remotely sensed imagery	Sentinel-1 SAR imagery	Copernicus Browser (https://browser.dataspace.copernicus.eu/)	Raster	10 m
			Sentinel-2 multispectral imagery	Copernicus Browser (https://browser.dataspace.copernicus.eu/)	Raster	10 m

14679671, 2026, 1, Downloaded from https://onlinelibrary.wiley.com/doi/10.1111/tgis.70190 by Serdar Selim - Akdeniz University , Wiley Online Library on [08/02/2026]. See the Terms and Conditions (https://onlinelibrary.wiley.com/terms-and-conditions) on Wiley Online Library for rules of use; OA articles are governed by the applicable Creative Commons License

studies published between 2019 and the first quarter of 2024 were reviewed. Following this literature review, only variables that appeared in 50% or more of the analyzed studies were selected as primary conditioning factors. It was observed that the most frequently used factors are slope, LULC, elevation, rainfall, distance from river, soil, and drainage density (Figure 1b). To create thematic maps for these seven factors, all data were processed in ArcGIS Pro and classified into five classes according to their flood triggering status. This method is the most frequently used classification method in the literature (Appendix B, Table B1). All maps were produced in raster format at the same resolution as the Advanced Land Observing Satellite Phased Array L-band SAR (ALOS PALSAR) Digital Elevation Model (DEM) data, at a 12.5 m resolution, and projected onto the World Geodetic System 1984 (WGS84) Universal Transverse Mercator (UTM) Zone 36N coordinate system.

Slope is an important factor in determining the rate and duration of water flow (Hagos et al. 2022; Ogato et al. 2020). Areas with little or no slope are more susceptible to flooding (M Amen et al. 2023). The slope map (in degrees) was produced from ALOS PALSAR DEM data using the Slope tool in ArcGIS (Figure 3a).

LULC directly affects infiltration rates and surface runoff (Belazreg et al. 2024; Hagos et al. 2022; M Amen et al. 2023). Forests and vegetation increase infiltration rates and decrease runoff rates. Therefore, forested and vegetated areas are less susceptible to flooding (Hagos et al. 2022; Souissi et al. 2020). Water bodies and residential areas, on the other hand, are more susceptible to flooding because they are impervious surfaces (Ogato et al. 2020). The LULC map was produced by classifying the CORINE Land Cover data (2018) in vector data format and using the Polygon to Raster tool in ArcGIS (Figure 3b). The standard Corine Land Cover (CLC) cover nomenclature includes 44 land cover classes. These are grouped into a three-level hierarchy. This study was conducted on the basis of CLC Level 1 in accordance with its purpose and scope. Level 1 consists of artificial surfaces, agricultural areas, forests and semi-natural areas, wetlands and water bodies (Heymann 1994).

Elevation plays an important role in the direction and depth of water flow (Hammami et al. 2019). Since the flow direction is from high to low elevation, low-elevation areas are more susceptible to flooding (Cabrera and Lee 2020; M Amen et al. 2023; Souissi et al. 2020). The elevation map was obtained by producing a mosaic image from a total of three ALOS PALSAR DEM data, which covered the entire study area, required as a result of the lack of a single DEM data covering the entire study area (Figure 3c).

Excessive rainfall in a short period of time is one of the most important factors influencing the occurrence of floods (M Amen et al. 2023). In this study, the total annual rainfall for each station was calculated by taking into account the monthly rainfall measured at a total of eight different meteorological stations within and surrounding the study area. A rainfall map was produced using the inverse distance weighting (IDW) method (Figure 3d), which is the most frequently used interpolation method in the literature (Appendix B, Table B1). This method is frequently preferred because it does not require many parameters that affect the interpolation results either positively or negatively; it has a simple mathematical background based directly on spatial autocorrelation due to the small number of sample points, and it has a high processing speed due to its low complexity.

The distance from a river is a critical factor in flood susceptibility, as the probability of flooding decreases as the distance increases (Cabrera and Lee 2020; M Amen et al. 2023). The distance from a river map was produced using the Euclidean Distance tool in ArcGIS, based on the active river network from OpenStreetMap (OSM) (Figure 3e).

Soil texture, structure, permeability and depth significantly affect its ability to be infiltrated, absorbing water (Hammami et al. 2019; Ogato et al. 2020). Soils with low permeability are more susceptible to flooding. In this study, the soil permeability map, produced by the Remote Sensing and Geographic Information Systems Graduate Program of Akdeniz University, based on information contained in a soil map prepared by the General Directorate of TOPRAKSU, was used directly (Figure 3f).

Drainage density is also reported as important in literature; calculated by dividing the total length of the river by the total area (Desalegn and Mulu 2021; Hagos et al. 2022). The higher the drainage density, the higher the risk of flooding (Osman and Das 2023; Rai et al. 2023; Souissi et al. 2020). The drainage density map was produced using the Line Density tool in ArcGIS, based on the active river network obtained from OSM (Figure 3g).

2.2.2 | Socioeconomic Factors Exposed to Flooding

In addition to the other data, population density, the area of farmland, road networks, historical and tourist attractions, as well as hotel locations were included to better inform an outline of susceptible areas and be able to assess the potential impacts.

Population density is an indicator of vulnerability to flooding (Ogato et al. 2020). To assess the potentially affected population, a density map was produced using the Kernel Density tool in ArcGIS Pro, integrating neighborhood-based population information from TURKSTAT (2024) with neighborhood settlement centers obtained from OSM (Figure 4a).

Although the coastal part of the study area is a tourist region, agricultural farmland activities are also carried out in the region. In order to assess the flood impact on fertile agricultural lands, the land capability classes in the soil map were directly included in this analysis, prepared by the General Directorate of TOPRAKSU (Figure 4b).

In the case of significant flood events, rapid transportation to the disaster area is an important factor. Major road network data were obtained from OSM to assess whether a potential flood disaster would disrupt transportation (Figure 4c). Due to the lack of accurate, complete, and reliable data on the power supply and communication network in the study area, these aspects could not be assessed.

14679671, 2026, 1, Downloaded from https://onlinelibrary.wiley.com/doi/10.1111/tgis.70190 by Serdar Selim - Akdeniz University , Wiley Online Library on [08/02/2026]. See the Terms and Conditions (https://onlinelibrary.wiley.com/terms-and-conditions) on Wiley Online Library for rules of use; OA articles are governed by the applicable Creative Commons License

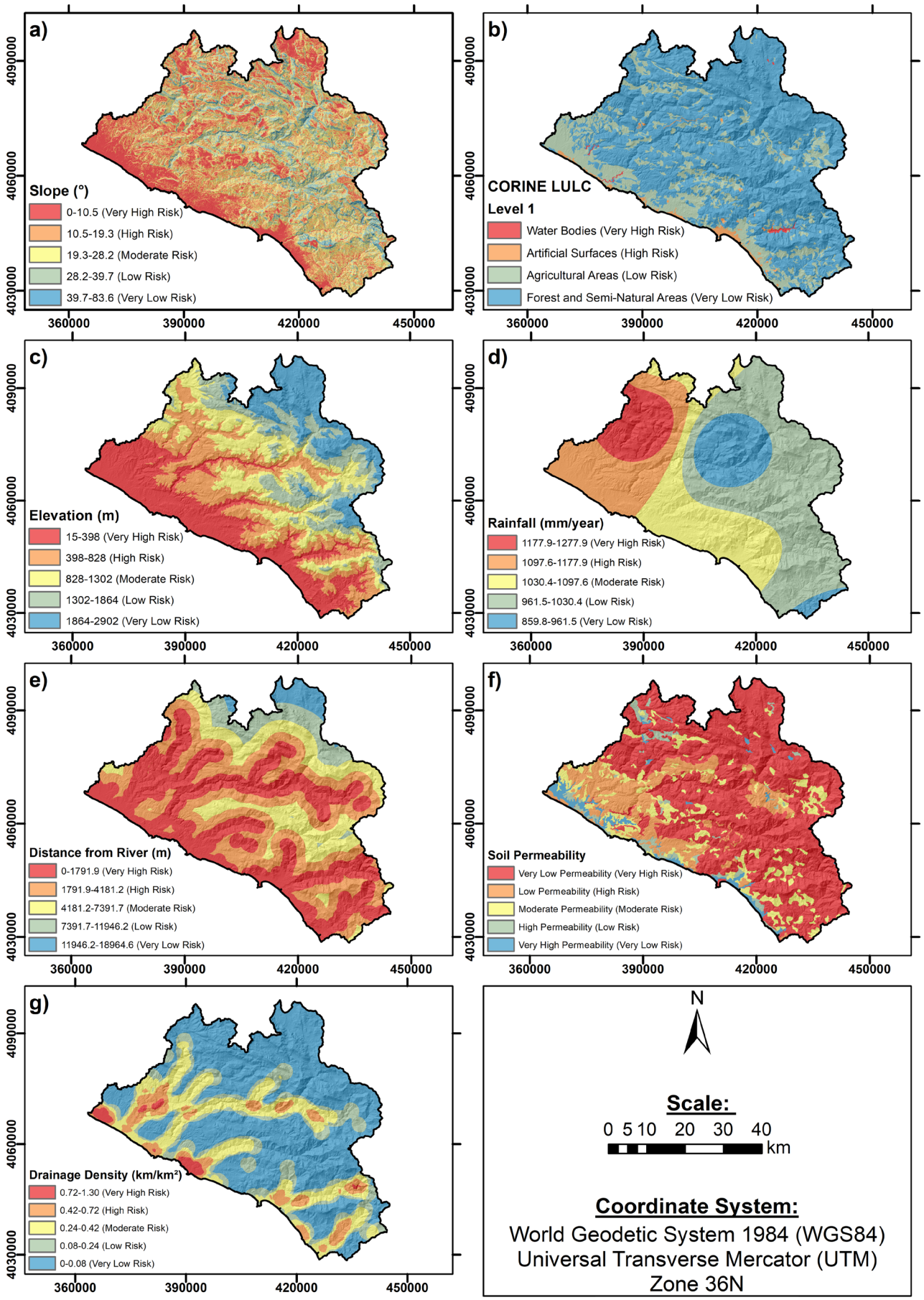


FIGURE 3 | Legend on next page.

14679671, 2026, 1, Downloaded from https://onlinelibrary.wiley.com/doi/10.1111/tgis.70190 by Serdar Selim - Akdeniz University , Wiley Online Library on [08/02/2026]. See the Terms and Conditions (https://onlinelibrary.wiley.com/terms-and-conditions) on Wiley Online Library for rules of use; OA articles are governed by the applicable Creative Commons License

FIGURE 3 | Thematic layers of flood conditioning factors: (a) slope; (b) land use/land cover (LULC); (c) elevation; (d) rainfall; (e) distance from river; (f) soil; (g) drainage density.

Given that tourism is the main source of livelihood and the population is concentrated in hotel locations especially during the summer season, data on historical and touristic places, cultural heritage and hotel locations were obtained from OSM to assess the potential impact of floods within the study area (Figure 4d).

2.2.3 | Validation Data

Due to the lack of spatial data on historical flood events, while previous studies that used only SAR or only multispectral satellite imagery (Dash and Sar 2020; Gahalod et al. 2024; Khan and Jhamnani 2024; Parajuli et al. 2023; Souissi et al. 2022), in this study SAR and multispectral satellite imagery were used together to produce a flood inventory map. The aim was to overcome the limitations of cloud cover in optical data and the potential overestimation of flood areas obtained from both sensors by using both sensors, thus creating a more robust flood inventory map for accuracy assessment.

All flood events that occurred in the study area in the last 5 years were investigated through national and local news sources. It was observed that at least one flood event occurred each year in the study area. However, suitable SAR and multispectral satellite imagery acquired simultaneously or close to each other for the same flood event could not be found due to the temporal resolution (or revisit frequency) of the satellite imagery and the adverse weather conditions with heavy clouds on the dates of the flood events. The primary challenge regarding the revisit frequency was not the direct theoretical cycle (5–6 days), but the practical availability of usable, synchronized data following a specific historical flood event. Because in many cases, the flood signature can diminish rapidly within a few days, making it difficult to find cloud-free optical images that coincide closely with both the SAR acquisition and the peak of the flood event.

In this study, data from recent years, which are more accurate and precise due to technological developments, were preferred. As a result of the investigations through the visualization interface in Copernicus Browser (https://browser.dataspace.copernicus.eu/), it was found appropriate to use Sentinel-1 SAR satellite imagery to map the inundated areas during the flood event of December 23–24, 2019, and Sentinel-2 multispectral satellite imagery to map the inundated areas during the flood event of November 25–26, 2023. These images were considered appropriate because they contain a high level of information about the flood due to reasons such as being taken 1 day after the flood and not including adverse weather conditions like clouds. Information on the satellite imagery used is given in Tables 2 and 3.

2.3 | Methodology

The flood susceptibility mapping and risk assessment was carried out in 4 main stages: (i) data collection, (ii) data preparation, (iii) analysis, and (iv) validation (Figure 5). While data collection and data preparation stages are detailed in Section 2.2, this section focuses on the AHP method used and the resulting flood susceptibility mapping in the analysis stage, and the validation stage of flood susceptibility mapping.

2.3.1 | Factor Weighting With AHP

Since the factors affecting flood formation have varying degrees of influence (Bhuyan et al. 2024; Hammami et al. 2019), the analytical hierarchy process (AHP) method proposed by Saaty (1980) was used to determine the relative weights of the selected factors. This method is widely preferred in flood susceptibility mapping due to its high accuracy, which generally exceeds 80% in similar studies (Ahmed et al. 2024; Gahalod et al. 2024; Ghosh et al. 2023; Khan and Jhamnani 2024; Nsangou et al. 2022). In this study, (i) based on expert opinions and literature (Hagos et al. 2022), a 7×7 pairwise comparison matrix was created according to Equation (1), assigning importance values between 1 (equal importance) and 9 (absolute importance) (Saaty 1977), as shown in Table 4.

$$A = \left[a_{ij}\right]_{n\times n} = \begin{bmatrix} a_{11} & a_{12} & \cdots & a_{1n} \\ a_{21} & a_{22} & \cdots & a_{2n} \\ \vdots & \vdots & \ddots & \vdots \\ a_{n1} & a_{n2} & \cdots & a_{nn} \end{bmatrix}, \quad a_{ii} = 1, \quad a_{ij} = 1/a_{ji}, \quad a_{ij} \neq 0 \tag{1}$$

After the pairwise comparison matrix is created, (ii) normalized weights are calculated by dividing each element value of the matrix by its total column value (Equation (2)) and then averaging the resulting row values for each factor (Equation (3)). The normalized pairwise comparison matrix and the weights calculated for each factor are shown in Table 5.

$$N_{ij} = \frac{A_{ij}}{\sum_{i=1}^{n} A_{ij}} \tag{2}$$

$$W_{ij} = \frac{\sum_{j=1}^{n} N_{ij}}{n} \tag{3}$$

where A_{ij} is the value of each element in the pairwise comparison matrix, N_{ij} is the value of each element in the normalized comparison matrix, and W_{ij} is the normalized weights of each factor.

Finally, (iii) the consistency of the matrix is evaluated using the Consistency Ratio (CR) in Equation (4). A CR value >0.1 indicates that the pairwise comparison matrix is too inconsistent to be reliable for analysis. Therefore, the CR value is expected to be equal to or <0.1.

$$CR = \frac{CI}{RI} \tag{4}$$

14679671, 2026, 1, Downloaded from https://onlinelibrary.wiley.com/doi/10.1111/tgis.70190 by Serdar Selim - Akdeniz University , Wiley Online Library on [08/02/2026]. See the Terms and Conditions (https://onlinelibrary.wiley.com/terms-and-conditions) on Wiley Online Library for rules of use; OA articles are governed by the applicable Creative Commons License

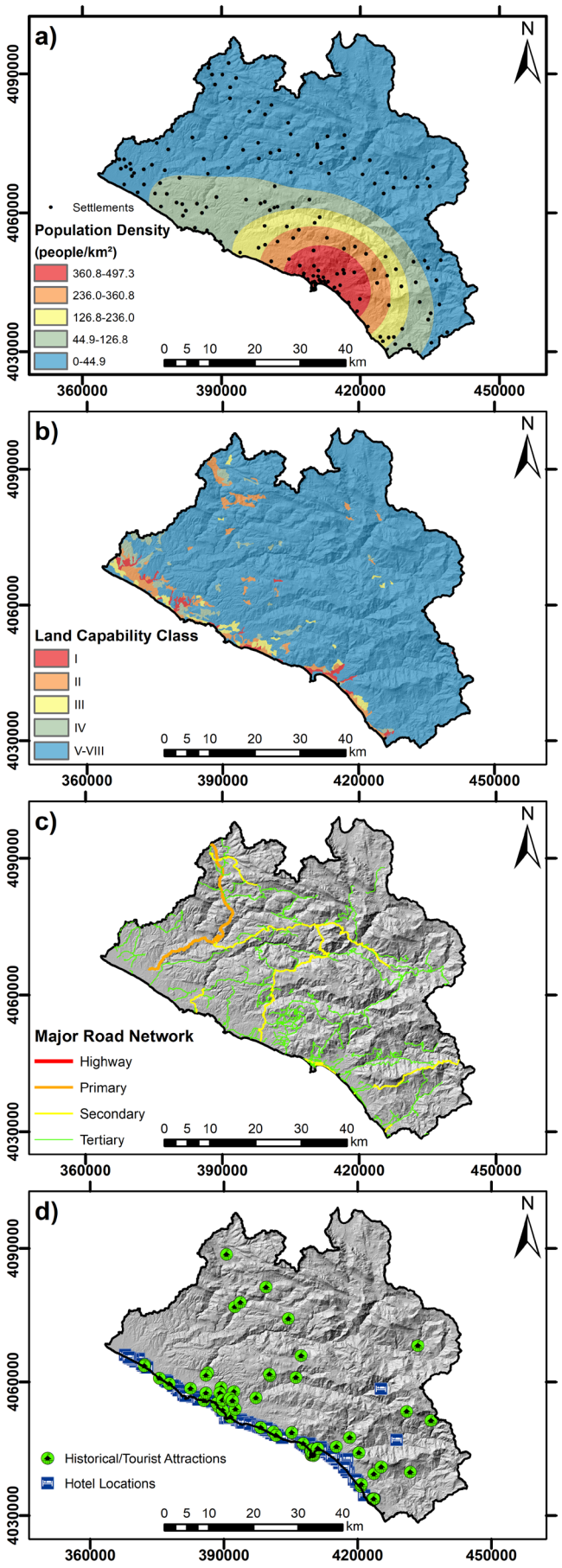


FIGURE 4 | Socioeconomic factors exposed to flooding: (a) population density; (b) land capability classes; (c) major road network; (d) historical/tourist attractions and hotel locations.

TABLE 2 | Characteristics of the SAR data used.

	Before flood	After flood
Platform	Sentinel-1B	Sentinel-1A
Instrument	SAR	SAR
Product level	Level-1 GRD	Level-1 GRD
Acquisition mode	IW	IW
Orbit direction	Ascending	Ascending
Relative orbit number	160	160
Sensing date	07.12.2019	25.12.2019
Sensing time (UTC)	15:49	15:50
Polarization used	VV	VV
Incidence angle (°)	30.54–46.19	30.57–46.17
Spatial resolution (m)	10	10

Abbreviations: GRD, ground range detected; IW, interferometric wide swath; UTC, coordinated universal time; VV, vertical transmit, vertical receive.

where CI is the Consistency Index calculated using Equation (5), and RI is the Random Index value that varies with the number of factors, which can be obtained from Saaty (1980).

$$CI = \frac{\lambda_{\max} - n}{n - 1} \tag{5}$$

where n is the number of factors (which is 7 for this study), and $\lambda_{\max}$ is the average value of the consistency vector, calculated using Equation (6).

$$\lambda_{\max} = \frac{\sum_{i=1}^{n} \frac{(AW)_i}{W_i}}{n} \tag{6}$$

where $(AW)_i$ is each value of the multiplication of the pairwise comparison matrix and normalized weights, and W_i is the normalized weights of each factor.

According to the above equations, it was calculated as $\lambda_{\max} = 7.37$, $CI = 0.06$, since $n = 7$, $RI = 1.32$ (Saaty 1980), and $CR = 0.05$. This means that the matrix is consistent and reliable, and therefore the calculated factor weightings are acceptable since $CR \leq 0.1$.

2.3.2 | Flood Susceptibility Mapping

After the weight of each factor was determined by AHP, and the classification and rating of each factor was made, the Flood Susceptibility Index (FSI) was calculated by using the Weighted Overlay tool in ArcGIS with the help of Equation (7); resulting in a map of flood susceptible areas. The cell values of the produced

14679671, 2026, 1, Downloaded from https://onlinelibrary.wiley.com/doi/10.1111/tgis.70190 by Serdar Selim - Akdeniz University , Wiley Online Library on [08/02/2026]. See the Terms and Conditions (https://onlinelibrary.wiley.com/terms-and-conditions) on Wiley Online Library for rules of use; OA articles are governed by the applicable Creative Commons License

TABLE 3 | Characteristics of the multispectral data used.

	Before flood		After flood	
Platform	Sentinel-2A		Sentinel-2B	
Instrument	MSI		MSI	
Product level	Level-2A		Level-2A	
Acquisition mode	INS-NOBS		INS-NOBS	
Orbit direction	Descending		Descending	
Relative orbit number	64		64	
Sensing date	23.10.2023		27.11.2023	
Sensing time (UTC)	08:40		08:41	
Tile ID	36SUF	36SVF	36SUF	36SVF
Cloud coverage (%)	0.00	0.01	0.02	7.79
Bands used	Green and SWIR channels (namely B3, B11)		Green and SWIR channels (namely B3, B11)	
Central wavelengths (nm)	559.8, 1613.7		559.0, 1610.4	
Spatial resolution (m)	10, 20		10, 20	

Abbreviations: INS-NOBS, nominal observation; MSI, multispectral instrument; SWIR, short-wave infrared.

flood susceptibility map vary between 1 and 5; areas with very low flood susceptibility represented by 1, and areas with very high flood susceptibility represented by 5. The classes and ratings of each factor and the corresponding weights are shown in Table 6.

$$FSI = \sum_{i=1}^{n} \left(W_i \times R_i \right) \tag{7}$$

where W_i is the weight of each factor, R_i is the rating of the factors, and n is the number of factors.

2.3.3 | Validation

To validate the flood susceptibility mapping, inundation maps were produced by thresholding, a method often used in the literature (Dash and Sar 2020; Gahalod et al. 2024; Khan and Jhamnani 2024; Parajuli et al. 2023; Souissi et al. 2022). In these inundation maps, similar areas representing inundated areas were identified and a flood inventory map was produced (Figure 6).

Because SAR satellite imagery can provide data on the Earth's surface day and night and in all weather conditions, it has a significant advantage in mapping inundated areas (Khan and Jhamnani 2024; Parajuli et al. 2023). Sentinel-1 Level-1 Ground Range Detected (GRD) products were used as SAR satellite imagery in this study (Table 2). The SeNtinel Applications Platform (SNAP) software (version 10.0.0) was used, and the following pre-processing steps were applied: (1) apply orbit file; (2) thermal noise removal; (3) radiometric calibration; (4) multilooking (the number of looks in the azimuth and range directions was 3×3, and the image was averaged in these directions to remove the speckle effect inherent in the SAR image); (5) Range-Doppler Terrain Correction (Shuttle Radar Topography Mission 1 arc-second Height [SRTM 1Sec HGT] DEM data were used). The resulting images were orthorectified to UTM/WGS84 projection and pixel spacings of the final products were adjusted to 10 m. (6) converting backscatter values from linear scale to logarithmic scale ($\sigma^0_{dB} = 10 \times \log 10\, \sigma^0$); (7) creating stack; and (8) subset. Then, (9) the pre- and post-flood images were compared to determine an appropriate threshold (a value of 5 was considered appropriate for this study). Areas where the difference between the two images (pre- and post-flood) was > 5 dB were mapped as inundated areas. (10) The resulting map was exported and imported into ArcGIS, and finally, (11) high elevation areas (areas with elevation classes 1 and 2) were masked to avoid mapping snow-covered areas as inundated areas. At this stage, the resolution of the masked raster data was downsampled to 12.5 m, the same resolution as the flood susceptibility map.

Figure 7a,b show the Dual Pol Ratio RGB images before and after the flood event that occurred on December 23–24, 2019. In these maps, water surfaces are represented in blue. Figure 7c shows the inundation map obtained after applying the threshold value. Since SAR data are sensitive to snow cover, and especially wet snow cover has a similar scattering mechanism to water surfaces (Tsai et al. 2019), this map shows snow cover in addition to inundated areas. The final inundation map with the masked snow cover is shown in Figure 7d.

Sentinel-2 Level-2A products, which are orthorectified to the UTM/WGS84 projection and radiometrically, geometrically, and atmospherically corrected, were used as multispectral satellite imagery (Table 3). Since the Modified Normalized Difference Water Index (MNDWI) is frequently used to map inundated areas from multispectral (or optical) satellite imagery (Dash and Sar 2020; Souissi et al. 2022), the following pre-processing steps were applied: (1) a mosaic image was produced from the two images acquired on the same date; (2) the SWIR band was resampled to the same resolution as the green band; (3) the image was clipped to reduce the processing time; (4) MNDWI values were calculated using Equation (8) (Xu 2006); (5) where a

14679671, 2026, 1, Downloaded from https://onlinelibrary.wiley.com/doi/10.1111/tgis.70190 by Serdar Selim - Akdeniz University , Wiley Online Library on [08/02/2026]. See the Terms and Conditions (https://onlinelibrary.wiley.com/terms-and-conditions) on Wiley Online Library for rules of use; OA articles are governed by the applicable Creative Commons License

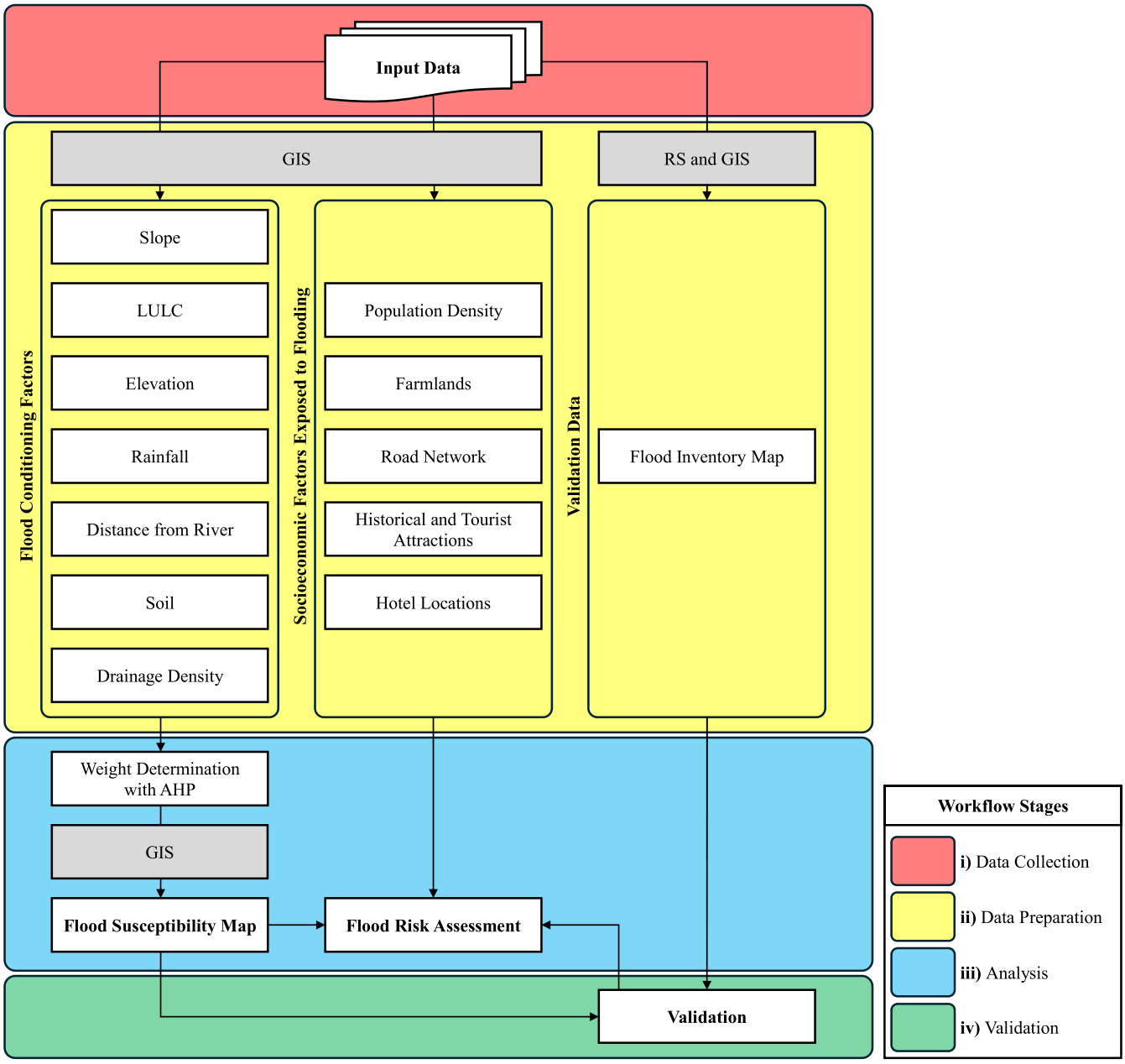


FIGURE 5 | Workflow diagram for flood susceptibility mapping and risk assessment.

TABLE 4 | Pairwise comparison matrix of seven flood conditioning factors.

Factors	Slope	Elevation	Drainage density	Distance from river	Rainfall	Soil	Land use/ Land cover
Slope	1	2	3	3	5	7	9
Elevation	1/2	1	2	3	5	7	9
Drainage density	1/3	1/2	1	2	3	5	7
Distance from river	1/3	1/3	1/2	1	3	5	7
Rainfall	1/5	1/5	1/3	1/3	1	3	5
Soil	1/7	1/7	1/5	1/5	1/3	1	3
Land use/Land cover	1/9	1/9	1/7	1/7	1/5	1/3	1
Sum	2.62	4.29	7.18	9.68	17.53	28.33	41.00

14679671, 2026, 1, Downloaded from https://onlinelibrary.wiley.com/doi/10.1111/tgis.70190 by Serdar Selim - Akdeniz University , Wiley Online Library on [08/02/2026]. See the Terms and Conditions (https://onlinelibrary.wiley.com/terms-and-conditions) on Wiley Online Library for rules of use; OA articles are governed by the applicable Creative Commons License

TABLE 5 | Normalized pairwise comparison matrix.

Factors	Slope	Elevation	Drainage density	Distance from river	Rainfall	Soil	Land use/ Land cover	Sum	Weights
Slope	0.38	0.47	0.42	0.31	0.29	0.25	0.22	2.33	0.33 (33%)
Elevation	0.19	0.23	0.28	0.31	0.29	0.25	0.22	1.76	0.25 (25%)
Drainage density	0.13	0.12	0.14	0.21	0.17	0.18	0.17	1.11	0.16 (16%)
Distance from river	0.13	0.08	0.07	0.10	0.17	0.18	0.17	0.90	0.13 (13%)
Rainfall	0.08	0.05	0.05	0.03	0.06	0.11	0.12	0.49	0.07 (7%)
Soil	0.05	0.03	0.03	0.02	0.02	0.04	0.07	0.26	0.04 (4%)
Land use/Land cover	0.04	0.03	0.02	0.01	0.01	0.01	0.02	0.15	0.02 (2%)
Sum	1.00	1.00	1.00	1.00	1.00	1.00	1.00	7.00	1.00 (100%)

$\lambda_{max} = 7.37$; CI = 0.06; RI = 1.32 (Saaty 1980)

CR = 0.05 ≤ 0.1.

threshold was applied to areas with MNDWI values > 0, assuming that positive values represent water surfaces in the resulting images. Areas that were represented as water surfaces in the post-flood image but not in the pre-flood image were mapped as inundated areas. Finally, (6) high elevation areas (areas with elevation classes 1 and 2) were masked to avoid mapping snow-covered areas as inundated areas. At this stage, the resolution of the masked raster data was downsampled to 12.5 m, the same resolution as the flood susceptibility map.

$$MNDWI = \frac{Green - SWIR}{Green + SWIR} \quad (8)$$

where *Green* is the Band 3 of the Sentinel-2 satellite image, *SWIR* is the Band 11 of the Sentinel-2 satellite image.

Figure 8a,b show True Color RGB images before and after the flood event that occurred on November 25–26, 2023. Figure 8c,d show the MNDWI images derived from the pre- and post-flood images. In these maps, water surfaces are represented in blue. Figure 8e shows the inundation map obtained after applying the threshold. The equation used for MNDWI (Equation (8)) was previously used by Dozier (1989) to extract snow cover, and similarly, Hall et al. (1995) used this equation to extract snow cover as the Normalized Difference Snow Index (NDSI). The final inundation map with the snow cover masked is shown in Figure 8f.

The inundation maps, produced separately from SAR and multispectral satellite imagery, had similar areas representing the inundated areas, so a flood inventory map could be reliably produced. In this way, the incorrectly mapped areas in the inundation maps produced from SAR and multispectral satellite imagery for the floods that occurred on two different dates were eliminated, and the most susceptible areas that were flooded on both dates were mapped. The validation of the flood susceptibility map was performed on a pixel basis using the produced flood inventory map.

3 | Results and Discussion

As a result of the pixel-based validation process, it was observed that no pixel in the flood inventory map is located in the very low susceptible area. 19 pixels (2.2%) are in the low susceptible area, while 41 pixels (4.6%) are in the medium susceptible area. 331 pixels (37.5%) are in the high susceptible area, while 491 pixels (55.7%) are in the very high susceptible area (Figure 9a,b). Therefore, 93.2% of the flood inventory map corresponds to high or very high susceptible areas, which is a very high accuracy. This accuracy is much more satisfactory than that obtained in other studies that have previously performed validation through satellite imagery (Allafta and Opp 2021; Dash and Sar 2020; Gahalod et al. 2024; Islam et al. 2022; Khan and Jhamnani 2024; Parajuli et al. 2023; Souissi et al. 2022). These results show the potential of the seven most frequently used factors in the literature and the AHP method to produce highly accurate and reliable flood susceptibility maps in areas with data scarcity. However, it should be noted that the threshold values used in the production of inundation maps, and thus flood inventory maps, may have an impact on the accuracy of the method. In addition, the fact that each study area has its own characteristics and how the factors to be included in the study for these specific characteristics affect the accuracy obtained is considered a problem that should be investigated in future studies.

It was determined that the most important flood conditioning factors in the region are slope, elevation, drainage density, and distance from river, and the least important factors are rainfall, soil, and LULC (Table 6). Since the flood conditioning factors and their weights may vary depending on the study area and expert knowledge, it is not possible to use the same factors or weights in all future studies. For example, if the main flood type in a region is river flooding, the most important factor is expected to be distance from river, as in Sakmongkoljit et al. (2021). Or, if rainfall in a region is highly variable, it is natural that the most important factor is rainfall, as in Arya and

14679671, 2026, 1, Downloaded from https://onlinelibrary.wiley.com/doi/10.1111/tgis.70190 by Serdar Selim - Akdeniz University , Wiley Online Library on [08/02/2026]. See the Terms and Conditions (https://onlinelibrary.wiley.com/terms-and-conditions) on Wiley Online Library for rules of use; OA articles are governed by the applicable Creative Commons License

TABLE 6 | Classes and ratings of the factors and corresponding weights.

Factors	Classes (Natural breaks/Jenks)	Descriptive level (Flood susceptibility)	Ratings (Ri)	Factor weights (Wi)	Class weights
Slope (°)	39.7–83.6	Very low risk	1	0.33	0.33
	28.2–39.7	Low risk	2		0.66
	19.3–28.2	Moderate risk	3		0.99
	10.5–19.3	High risk	4		1.32
	0–10.5	Very high risk	5		1.65
Elevation (m)	1864–2902	Very low risk	1	0.25	0.25
	1302–1864	Low risk	2		0.50
	828–1302	Moderate risk	3		0.75
	398–828	High risk	4		1.00
	15–398	Very high risk	5		1.25
Drainage density (km/km^2)	0–0.08	Very low risk	1	0.16	0.16
	0.08–0.24	Low risk	2		0.32
	0.24–0.42	Moderate risk	3		0.48
	0.42–0.72	High risk	4		0.64
	0.72–1.30	Very high risk	5		0.80
Distance from river (m)	11,946.2–18,964.6	Very low risk	1	0.13	0.13
	7391.7–11,946.2	Low risk	2		0.26
	4181.2–7391.7	Moderate risk	3		0.39
	1791.9–4181.2	High risk	4		0.52
	0–1791.9	Very high risk	5		0.65
Rainfall (mm/year)	859.8–961.5	Very low risk	1	0.07	0.07
	961.5–1030.4	Low risk	2		0.14
	1030.4–1097.6	Moderate risk	3		0.21
	1097.6–1177.9	High risk	4		0.28
	1177.9–1277.9	Very high risk	5		0.35
Soil	Very high permeability	Very low risk	1	0.04	0.04
	High permeability	Low risk	2		0.08
	Moderate permeability	Moderate risk	3		0.12
	Low permeability	High risk	4		0.16
	Very low permeability	Very high risk	5		0.20
Land use/Land cover	Forest and semi-natural areas	Very low risk	1	0.02	0.02
	Agricultural areas	Low risk	2		0.04
	Artificial surfaces	High risk	4		0.08
	Water bodies	Very high risk	5		0.10

14679671, 2026, 1, Downloaded from https://onlinelibrary.wiley.com/doi/10.1111/tgis.70190 by Serdar Selim - Akdeniz University , Wiley Online Library on [08/02/2026]. See the Terms and Conditions (https://onlinelibrary.wiley.com/terms-and-conditions) on Wiley Online Library for rules of use; OA articles are governed by the applicable Creative Commons License

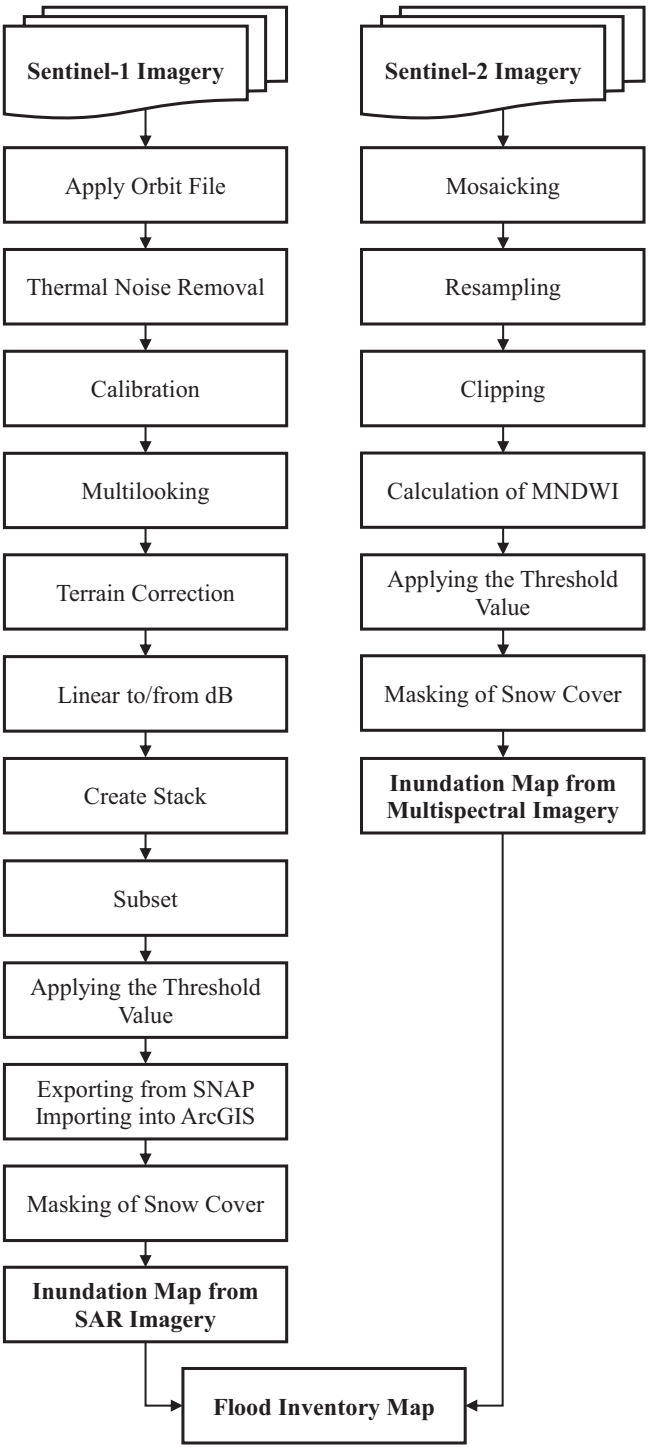


FIGURE 6 | Workflow diagram for producing the flood inventory map used in the validation stage.

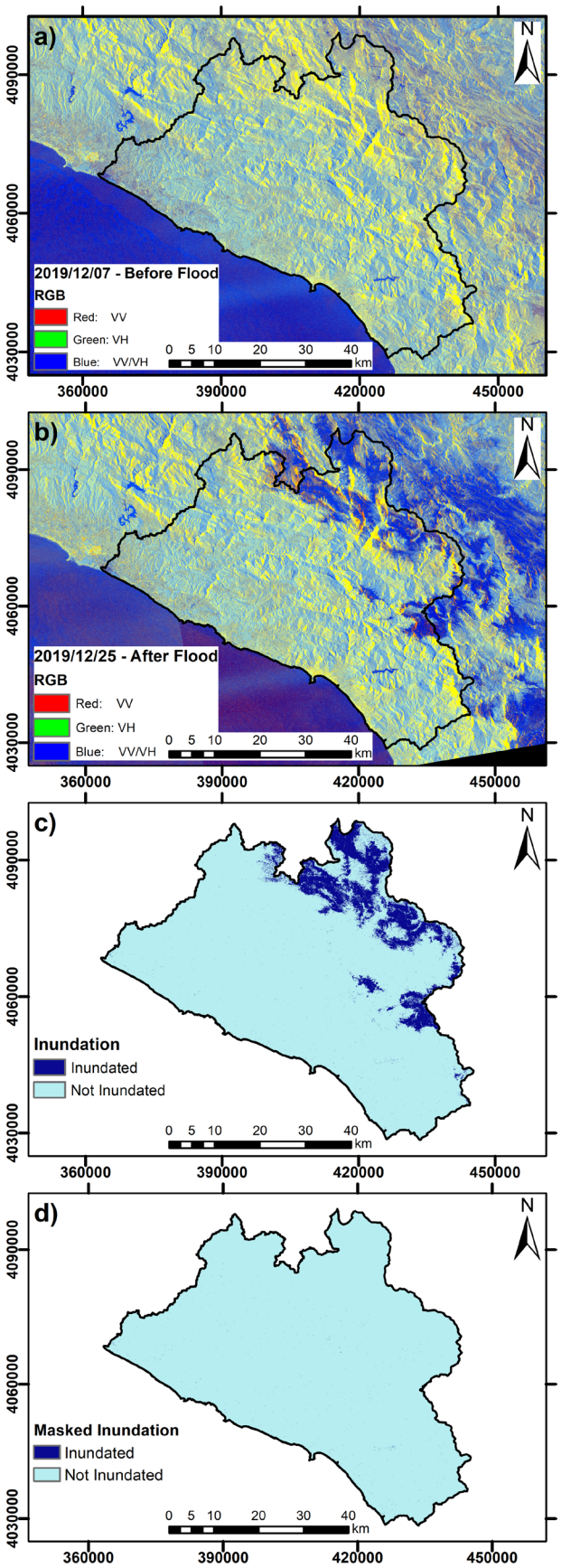


FIGURE 7 | Maps derived from synthetic aperture radar (SAR) satellite imagery: (a) pre-flood RGB image; (b) post-flood RGB image; (c) inundation map; (d) final inundation map with snow-covered areas masked.

Singh (2021) and Chukwuma et al. (2021). If the study area is flat, as in Ali et al. (2019) and Waqas et al. (2021), factors such as rainfall, distance from river, LULC, and soil are likely to have a much greater contribution than factors such as slope and elevation. In this study region, slope and elevation were found to be the most important factors in the occurrence of flooding, especially due to the changes in the topographic structure (Aydin and Iban 2023; Daneshparvar et al. 2022; Gahalod et al. 2024; Msabi and Makonyo 2021; Rahman et al. 2023). While their influence on flood occurrence may vary due to regional characteristics, it

14679671, 2026, 1, Downloaded from https://onlinelibrary.wiley.com/doi/10.1111/tgis.70190 by Serdar Selim - Akdeniz University , Wiley Online Library on [08/02/2026]. See the Terms and Conditions (https://onlinelibrary.wiley.com/terms-and-conditions) on Wiley Online Library for rules of use; OA articles are governed by the applicable Creative Commons License

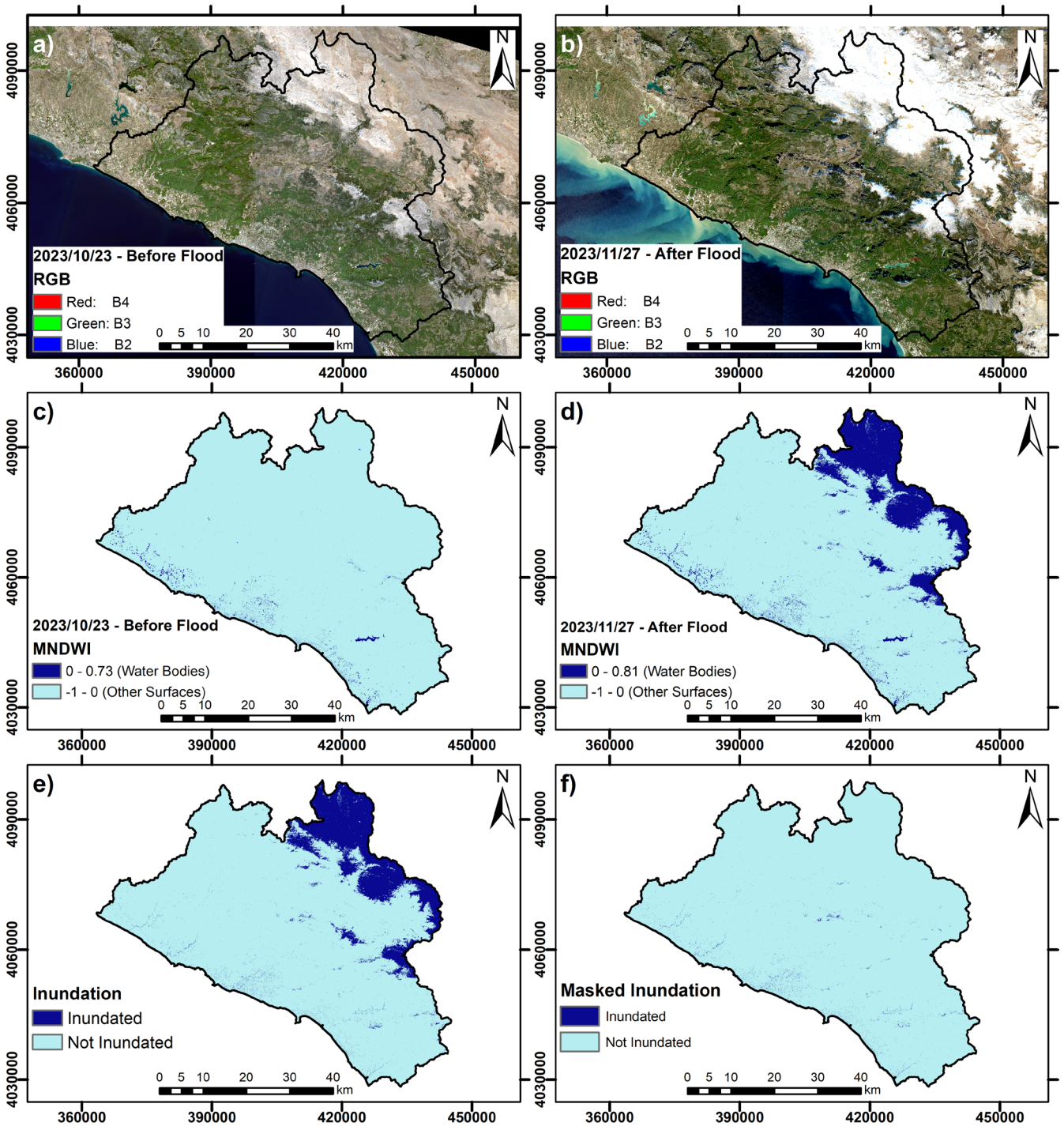


FIGURE 8 | Maps derived from multispectral satellite imagery: (a) pre-flood RGB image; (b) post-flood RGB image; (c) pre-flood Modified Normalized Difference Water Index (MNDWI) map; (d) post-flood MNDWI map; (e) inundation map; (f) final inundation map with snow-covered areas masked.

is an undeniable fact that these seven factors encompass most of the relevant aspects of flooding across the globe.

Similar to the flood susceptibility map (Figure 9a), it is observed that the inundated areas in the flood inventory map are concentrated near the coastal areas and rivers where the slope and elevation are low, and the soils in these areas are mostly the most impermeable. Most of the study area has moderate flood susceptibility (42.8%), 30.9% has high flood susceptibility, 4.2% has very high flood susceptibility, 21.4% has low flood susceptibility, and 0.7% has very low flood susceptibility (Figure 9c). The high and very high susceptibility areas represent up to 35.1% of the study area (1048.6 km^2). It can be seen that the high and very high susceptibility areas are concentrated in the coastal areas, where the slope and elevation are low, and it is close to the rivers, where the soils in these areas are the most impermeable (Figure 9a) (Allafta and Opp 2021; Aydin and Iban 2023; Chukwu et al. 2023; Ebodé et al. 2024; Fatah et al. 2022;

14679671, 2026, 1, Downloaded from https://onlinelibrary.wiley.com/doi/10.1111/tgis.70190 by Serdar Selim - Akdeniz University , Wiley Online Library on [08/02/2026]. See the Terms and Conditions (https://onlinelibrary.wiley.com/terms-and-conditions) on Wiley Online Library for rules of use; OA articles are governed by the applicable Creative Commons License

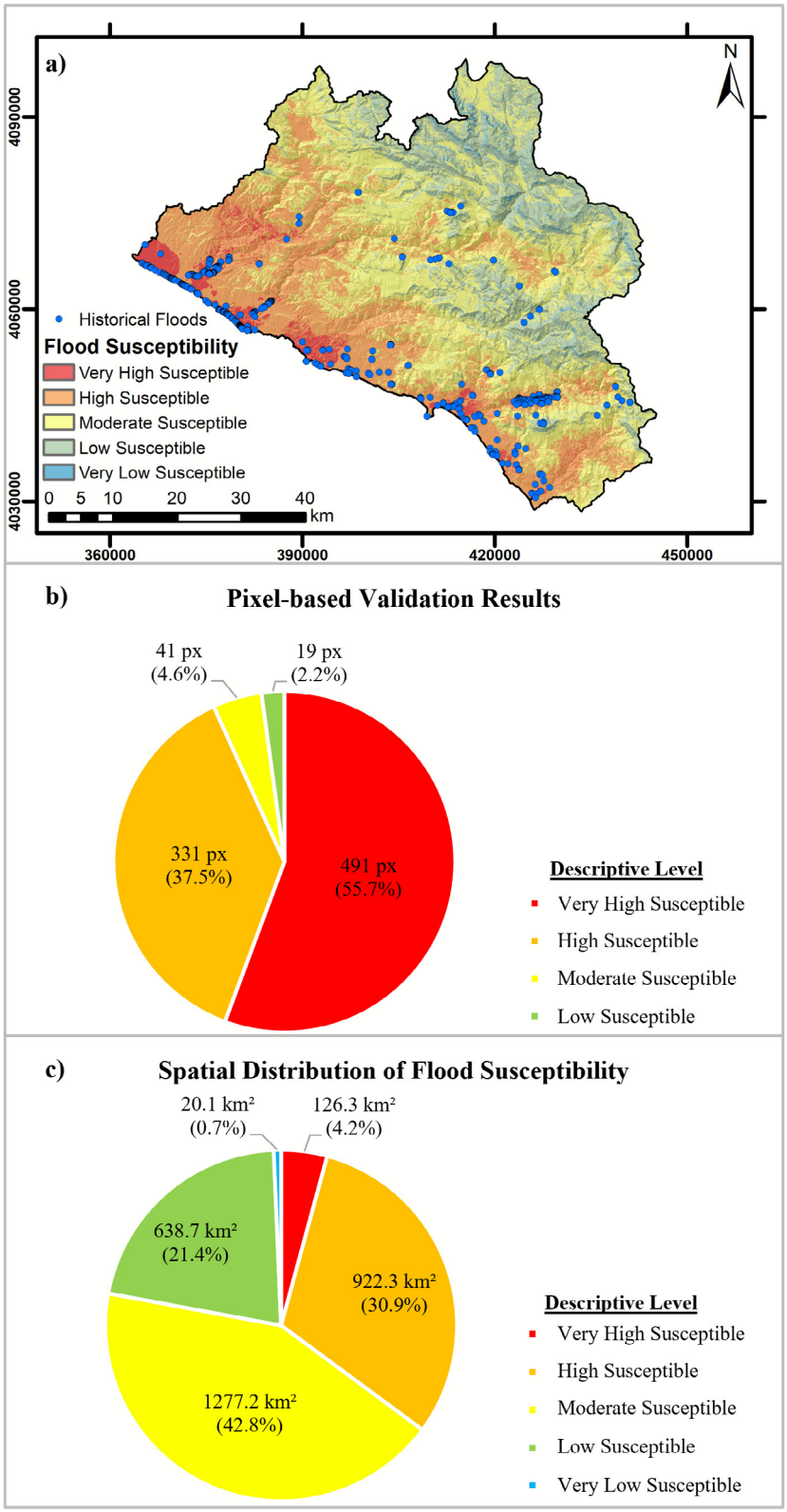


FIGURE 9 | (a) Point-based representation of the flood inventory map on the flood susceptibility map; (b) pixel-based validation results; (c) spatial distribution of flood susceptibility.

Karymbalis et al. 2021; Lin et al. 2019; Souissi et al. 2020; Ullah and Zhang 2020).

The produced flood susceptibility map was overlaid with physical and socioeconomic factor data, and pixel-based analyses were performed. According to the findings, 91.6% (42.5 km^2) of the urban areas and 68.7% (452.3 km^2) of the agricultural areas are highly or very highly susceptible. These results emphasize that urban and agricultural areas are the most vulnerable to flooding (Allafta and Opp 2021; Dash and Sar 2020; Desalegn

14679671, 2026, 1, Downloaded from https://onlinelibrary.wiley.com/doi/10.1111/tgis.70190 by Serdar Selim - Akdeniz University , Wiley Online Library on [08/02/2026]. See the Terms and Conditions (https://onlinelibrary.wiley.com/terms-and-conditions) on Wiley Online Library for rules of use; OA articles are governed by the applicable Creative Commons License

and Mulu 2021). On the other hand, high elevation and sloping areas with low drainage density were found to be of low or very low susceptibility (Aydin and Sevgi Birincioğlu 2022; Chaulagain et al. 2023; Chukwu et al. 2023; Fatah et al. 2022). These areas are mostly characterized by forested areas with low rainfall (Chukwu et al. 2023).

In the most densely populated area (360.8–497.3 people/km^2), 60.7% has high or very high susceptibility to flooding (92.02 km^2). In the second most densely populated area (236.0–360.8 people/km^2), this rate is 50.0% (90.86 km^2). If the areas with a high or very high flood susceptibility in these densely populated areas are considered together, the ratio is 54.8% (182.88 km^2). This indicates that more than half of these densely populated areas are susceptible and shows the population density that could be most affected by a possible flood disaster in the region.

It was observed that 68.7% (452.3 km^2) of the agricultural land in the region is at high or very high susceptibility, and 19.2% (86.6 km^2) of these agricultural lands are Class I (5.7%) and Class II (13.5%) soils. These agricultural lands can be considered as lands that can be easily cultivated and produced productively because they have minimal constraints. A possible flood disaster is likely to affect the crops in these agricultural lands and thus the farmers.

50.9% of the major road network in the study area is in a high susceptible area, and 11.3% is at very high susceptibility. It is noticeable that both the main highway and the major roads are susceptible. This shows that a possible flood disaster could considerably disrupt transportation. In such a case, rescue teams may have to use alternate routes to reach the area, which may delay reaching the disaster area and may lead to an increase in loss of life or property.

58.7% (44 places) of the historical and tourist attractions in the study area are in the high susceptible and 26.7% (20 places) are in the very high susceptible. Therefore, 85.4% of the historical and tourist attractions are located in high or very high susceptible. A possible flood disaster during the tourist season could have a major impact on the tourism sector, which could seriously disrupt the regional economy.

48.9% (132 hotels) of the hotels in the study area are located in a highly susceptible area, and 50.7% (137 hotels) are located in very high susceptibility. This shows that almost all hotels in the region (99.6%) are located in high or very high susceptibility. Therefore, considering the population density in these hotels, where occupancy rates increase even more during the tourist season, in addition to the population of the region, a possible flood disaster during the tourist season could affect many people materially and morally.

The findings suggest a critical vulnerability for the Alanya Sub-Basin: the low-elevation coastal zones that facilitate the region's intense tourism and agricultural activities are the same areas identified as being under the highest flood susceptibility. This study reveals that the nature of flood events in the region is intrinsically linked to its development pattern, where nearly all major touristic infrastructure and productive lands are geographically fixed within these high-susceptibility zones. Unlike typical inland basins, a potential flood in this region presents a dual challenge: an immediate threat to a large seasonal population and a long-term risk to the core economic pillars of the sub-basin. Therefore, reducing disaster impacts requires a strategic shift toward integrated spatial planning that balances rapid urbanization with the hydrological realities of the Dim and Oba river systems.

Considering that 91.6% of the urban areas in the study area are at high or very high susceptibility, and that the population density in these areas is quite high, it is suggested that appropriate infrastructure works should be carried out urgently to reduce the possible destructive effects of the disaster and to prevent loss of life and property. Along with traditional engineering solutions, nature-based solutions (NbS) and green infrastructure, such as sustainable drainage systems and urban wetlands, should be integrated into urban planning to enhance flood resilience. As there is no airport or railway network in the region, it is essential to identify alternate routes or establish new routes to prevent transportation disruptions in the event of a flood disaster. This is to ensure smooth access and evacuation from the region. Furthermore, establishing a multi-layered flood governance framework that ensures seamless coordination between local authorities, stakeholders, and government agencies, along with community training programs, is vital to ensure coordinated evacuation and long-term disaster preparedness. In addition, improvements to drainage systems in agricultural areas would likely help to prevent crop loss, and plans should be made to protect cultural heritage sites at high or very high flood susceptibility.

4 | Conclusion

This study mapped flood susceptible areas and assessed potential impacts in a densely populated touristic sub-basin where spatial data on historical flood events are scarce. By employing the GIS-based AHP method with primary conditioning factors identified from an extensive literature review, the research provides a strategic framework for disaster management. The main conclusions can be summarized as follows:

The analysis reveals that slope and elevation are the most critical factors influencing flood susceptibility in this topographic structure. High and very high-susceptibility areas are primarily concentrated in low-lying coastal zones and near river networks. Notably, the study area's socioeconomic heart is under significant threat, as the vast majority of urban centers and productive agricultural lands are located within these high-susceptibility zones.

The vulnerability of the tourism sector is particularly remarkable, with nearly all hotel infrastructures and the majority of historical and tourist attractions situated in areas of high or very high susceptibility. Furthermore, the potential for transportation disruption is high, as a significant portion of the major road network is exposed to these susceptibility levels.

The high validation accuracy of 93.2%, obtained through the flood inventory map created using SAR and multispectral

14679671, 2026, 1, Downloaded from https://onlinelibrary.wiley.com/doi/10.1111/tgis.70190 by Serdar Selim - Akdeniz University , Wiley Online Library on [08/02/2026]. See the Terms and Conditions (https://onlinelibrary.wiley.com/terms-and-conditions) on Wiley Online Library for rules of use; OA articles are governed by the applicable Creative Commons License

satellite imagery, confirms that the AHP method remains a reliable and robust tool for regions with data scarcity. These results further demonstrate that the seven most frequently used conditioning factors in the literature (slope, LULC, elevation, rainfall, distance from river, soil, and drainage density) are highly effective in producing reliable susceptibility maps worldwide.

The structural overlap between high-value socioeconomic assets and flood-prone zones underscores that flood management in the region cannot be limited to traditional engineering. Instead, these findings emphasize the urgent need for a transition from reactive measures to proactive integrated spatial planning that prioritizes long-term resilience. Beyond traditional infrastructure, incorporating nature-based solutions, green infrastructure, and multi-layered governance frameworks is vital for enhancing the long-term resilience of the Alanya Sub-Basin.

Acknowledgments

The authors would like to thank the staff of Akdeniz University, Remote Sensing and Geographic Information Systems Graduate Program for their help in providing the data used in the study.

Funding

The authors have nothing to report.

Conflicts of Interest

The authors declare no conflicts of interest.

Data Availability Statement

The data that support the findings of this study are available from the corresponding author upon reasonable request.

References

Abdelgawad, A. G., E. Helal, M. F. Sobeih, and H. Elsayed. 2024. "Flood Hazard Mapping Using a GIS-Based Morphometric Analysis Approach in Arid Regions, a Case Study in the Red Sea Region, Egypt." *Applied Water Science* 14, no. 4: 81. https://doi.org/10.1007/s13201-024-02130-5.

Abdo, H. G. 2020. "Evolving a Total-Evaluation Map of Flash Flood Hazard for Hydro-Prioritization Based on Geohydromorphometric Parameters and GIS–RS Manner in Al-Hussain River Basin, Tartous, Syria." *Natural Hazards* 104, no. 1: 681–703. https://doi.org/10.1007/s11069-020-04186-3.

Abdulalim, A. A., and T. A. El Damaty. 2022. "Implementation of Remote Sensing and GIS Techniques to Study the Flash Flood Risk at NEOM Mega-City, Saudi Arabia." *Advances in Remote Sensing* 11, no. 4: 121–157. https://doi.org/10.4236/ars.2022.114008.

Ahmed, I., N. Das (Pan), J. Debnath, M. Bhowmik, and S. Bhattacharjee. 2024. "Flood Hazard Zonation Using GIS-Based Multi-Parametric Analytical Hierarchy Process." *Geosystems and Geoenvironment* 3, no. 2: 100250. https://doi.org/10.1016/j.geogeo.2023.100250.

Ajjur, S. B., and Y. K. Mogheir. 2020. "Flood Hazard Mapping Using a Multi-Criteria Decision Analysis and GIS (Case Study Gaza Governorate, Palestine)." *Arabian Journal of Geosciences* 13, no. 2: 44. https://doi.org/10.1007/s12517-019-5024-6.

Akdeniz, H. B., and E. C. Tuzcu. 2023. "Flood Risk Assessment and Mapping: A Case Study of the Aksu River Basin (Giresun), Türkiye." *Intercontinental Geoinformation Days* 6: 61–64.

Aksoy, H. 2023. "Flood Risk Analysis With AHP and the Role of Forests in Natural Flood Management: A Case Study From the North of Türkiye." *Kastamonu Üniversitesi Orman Fakültesi Dergisi* 23, no. 3: 282–297. https://doi.org/10.17475/kastorman.1394958.

Al-Areeq, A., S. Abba, M. Yassin, M. Benaafi, M. Ghaleb, and I. Aljundi. 2022. "Computational Machine Learning Approach for Flood Susceptibility Assessment Integrated With Remote Sensing and GIS Techniques From Jeddah, Saudi Arabia." *Remote Sensing* 14, no. 21: 5515. https://doi.org/10.3390/rs14215515.

Alarifi, S. S., M. Abdelkareem, F. Abdalla, and M. Alotaibi. 2022. "Flash Flood Hazard Mapping Using Remote Sensing and GIS Techniques in Southwestern Saudi Arabia." *Sustainability* 14, no. 21: 14145. https://doi.org/10.3390/su142114145.

Alharbi, T. 2023. "Mapping of Groundwater, Flood, and Drought Potential Zones in Neom, Saudi Arabia, Using GIS and Remote Sensing Techniques." *Water* 15, no. 5: 966. https://doi.org/10.3390/w15050966.

Ali, S. A., R. Khatun, A. Ahmad, and S. N. Ahmad. 2019. "Application of GIS-Based Analytic Hierarchy Process and Frequency Ratio Model to Flood Vulnerable Mapping and Risk Area Estimation at Sundarban Region, India." *Modeling Earth Systems and Environment* 5, no. 3: 1083–1102. https://doi.org/10.1007/s40808-019-00593-z.

Ali, S. A., F. Parvin, Q. B. Pham, et al. 2020. "GIS-Based Comparative Assessment of Flood Susceptibility Mapping Using Hybrid Multi-Criteria Decision-Making Approach, Naïve Bayes Tree, Bivariate Statistics and Logistic Regression: A Case of Topľa Basin, Slovakia." *Ecological Indicators* 117: 106620. https://doi.org/10.1016/j.ecolind.2020.106620.

Alimi, S. A., E. O. Oriola, S. S. Senbore, et al. 2023. "GIS-Assisted Flood-Risk Potential Mapping of Ilorin and Its Environs, Kwara State, Nigeria." *Remote Sensing in Earth Systems Sciences* 6, no. 3–4: 239–253. https://doi.org/10.1007/s41976-023-00093-w.

Allafta, H., and C. Opp. 2021. "GIS-Based Multi-Criteria Analysis for Flood Prone Areas Mapping in the Trans-Boundary Shatt Al-Arab Basin, Iraq-Iran." *Geomatics, Natural Hazards and Risk* 12, no. 1: 2087–2116. https://doi.org/10.1080/19475705.2021.1955755.

Aprillya, M. R., and U. Chasanah. 2022. "GIS Flood Prone Agricultural Land East Java Using Multi-Method Attribute Utility Theory." *MATRIK: Jurnal Manajemen, Teknik Informatika Dan Rekayasa Komputer* 22, no. 1: 117–128. https://doi.org/10.30812/matrik.v22i1.1511.

Argaz, A., B. Ouahman, A. Darkaoui, H. Bikhtar, E. Ayouch, and R. Lazaar. 2019. "Flood Hazard Mapping Using Remote Sensing and GIS Tools: A Case Study of Souss Watershed." *Journal of Materials and Environmental Science* 10, no. 2: 170–181. http://www.jmaterenvironsci.com.

Arya, A. K., and A. P. Singh. 2021. "Multi Criteria Analysis for Flood Hazard Mapping Using GIS Techniques: A Case Study of Ghaghara River Basin in Uttar Pradesh, India." *Arabian Journal of Geosciences* 14, no. 8: 656. https://doi.org/10.1007/s12517-021-06971-1.

Aslan, V. 2023. "Evaluation of Birecik Basin Flood Detection With GIS Assisted AHP Methods." *KSCE Journal of Civil Engineering* 27, no. 7: 2891–2907. https://doi.org/10.1007/s12205-023-1271-x.

Aydin, H. E., and M. C. Iban. 2023. "Predicting and Analyzing Flood Susceptibility Using Boosting-Based Ensemble Machine Learning Algorithms With SHapley Additive exPlanations." *Natural Hazards* 116, no. 3: 2957–2991. https://doi.org/10.1007/s11069-022-05793-y.

Aydin, M. C., and E. Sevgi Birincioğlu. 2022. "Flood Risk Analysis Using Gis-Based Analytical Hierarchy Process: A Case Study of Bitlis Province." *Applied Water Science* 12, no. 6: 122. https://doi.org/10.1007/s13201-022-01655-x.

14679671, 2026, 1, Downloaded from https://onlinelibrary.wiley.com/doi/10.1111/tgis.70190 by Serdar Selim - Akdeniz University , Wiley Online Library on [08/02/2026]. See the Terms and Conditions (https://onlinelibrary.wiley.com/terms-and-conditions) on Wiley Online Library for rules of use; OA articles are governed by the applicable Creative Commons License

Ayenew, W. A., and H. A. Kebede. 2023. "GIS and Remote Sensing Based Flood Risk Assessment and Mapping: The Case of Dikala Watershed in Kobo Woreda Amhara Region, Ethiopia." *Environmental and Sustainability Indicators* 18: 100243. https://doi.org/10.1016/j.indic.2023.100243.

Bansal, N., M. Mukherjee, and A. Gairola. 2022. "Evaluating Urban Flood Hazard Index (UFHI) of Dehradun City Using GIS and Multi-Criteria Decision Analysis." *Modeling Earth Systems and Environment* 8, no. 3: 4051–4064. https://doi.org/10.1007/s40808-021-01348-5.

Bansal, N., M. Mukherjee, and A. Gairola. 2023. "GIS-Based Multi-Criteria Decision Analysis for Mapping Flood-Prone Areas in Dehradun City, India." *Arabian Journal of Geosciences* 16, no. 9: 501. https://doi.org/10.1007/s12517-023-11605-9.

Baykal, T., E. Şener, and Ö. Terzi. 2023. "Application of Analytical Hierarchy Process for Flood Risk Analysis: A Case Study in Küçük Aksu River Basin (Antalya, Turkey)." *Iranian Journal of Science and Technology, Transactions of Civil Engineering* 47, no. 4: 2449–2466. https://doi.org/10.1007/s40996-023-01055-4.

Belazreg, N. E. H., M. Hasbaia, Z. Şen, and A. Ferhati. 2024. "Flood Risk Mapping Using Multi-Criteria Analysis (MCA) Through AHP Method Case of El-Ham Wadi Watershed of Hodna Basin (Algeria)." *Natural Hazards* 120, no. 2: 1023–1039. https://doi.org/10.1007/s11069-023-06239-9.

Bhuyan, M. J., N. Deka, and A. Saikia. 2024. "Micro-Spatial Flood Risk Assessment in Nagaon District, Assam (India) Using GIS-Based Multi-Criteria Decision Analysis (MCDA) and Analytical Hierarchy Process (AHP)." *Risk Analysis* 44, no. 4: 817–832. https://doi.org/10.1111/risa.14191.

Burayu, D. G., S. Karuppannan, and G. Shuniye. 2023. "Identifying Flood Vulnerable and Risk Areas Using the Integration of Analytical Hierarchy Process (AHP), GIS, and Remote Sensing: A Case Study of Southern Oromia Region." *Urban Climate* 51: 101640. https://doi.org/10.1016/j.uclim.2023.101640.

Cabrera, J. S., and H. S. Lee. 2019. "Flood-Prone Area Assessment Using GIS-Based Multi-Criteria Analysis: A Case Study in Davao Oriental, Philippines." *Water* 11, no. 11: 2203. https://doi.org/10.3390/w11112203.

Cabrera, J. S., and H. S. Lee. 2020. "Flood Risk Assessment for Davao Oriental in The Philippines Using Geographic Information System-Based Multi-Criteria Analysis and the Maximum Entropy Model." *Journal of Flood Risk Management* 13, no. 2. https://doi.org/10.1111/jfr3.12607.

Cai, S., J. Fan, and W. Yang. 2021. "Flooding Risk Assessment and Analysis Based on GIS and the TFN-AHP Method: A Case Study of Chongqing, China." *Atmosphere* 12, no. 5: 623. https://doi.org/10.3390/atmos12050623.

Chakraborty, S., and S. Mukhopadhyay. 2019. "Assessing Flood Risk Using Analytical Hierarchy Process (AHP) and Geographical Information System (GIS): Application in Coochbehar District of West Bengal, India." *Natural Hazards* 99, no. 1: 247–274. https://doi.org/10.1007/s11069-019-03737-7.

Chaulagain, D., P. Ram Rimal, S. N. Ngando, B. E. K. Nsafon, D. Suh, and J.-S. Huh. 2023. "Flood Susceptibility Mapping of Kathmandu Metropolitan City Using GIS-Based Multi-Criteria Decision Analysis." *Ecological Indicators* 154: 110653. https://doi.org/10.1016/j.ecolind.2023.110653.

Chen, Y. 2022. "Flood Hazard Zone Mapping Incorporating Geographic Information System (GIS) and Multi-Criteria Analysis (MCA) Techniques." *Journal of Hydrology* 612: 128268. https://doi.org/10.1016/j.jhydrol.2022.128268.

Chukwu, M., X. Huang, B. Peng, and I. Oloruntimilehin. 2023. "Flood Risk Evaluation Using AHP-Based Model and GIS Technique: A Case Study of Ethiope East and West Local Government Areas, Nigeria." *Journal of the Indian Society of Remote Sensing* 51, no. 12: 2561–2576. https://doi.org/10.1007/s12524-023-01786-x.

Chukwuma, E. C., C. C. Okonkwo, J. O. Ojediran, D. C. Anizoba, J. I. Ubah, and C. P. Nwachukwu. 2021. "A GIS Based Flood Vulnerability Modelling of Anambra State Using an Integrated IVFRN-DEMATEL-ANP Model." *Heliyon* 7, no. 9: e08048. https://doi.org/10.1016/j.heliyon.2021.e08048.

CORINE Land Cover. 2018. "(vector/raster 100 m), Europe, 6-yearly." https://doi.org/10.2909/71c95a07-e296-44fc-b22b-415f42acfdf0.

Costache, R. 2019. "Flood Susceptibility Assessment by Using Bivariate Statistics and Machine Learning Models—A Useful Tool for Flood Risk Management." *Water Resources Management* 33, no. 9: 3239–3256. https://doi.org/10.1007/s11269-019-02301-z.

Costache, R., A. Arabameri, I. Costache, et al. 2022. "Flood Susceptibility Evaluation Through Deep Learning Optimizer Ensembles and GIS Techniques." *Journal of Environmental Management* 316: 115316. https://doi.org/10.1016/j.jenvman.2022.115316.

Daneshparvar, B., S. Rasi Nezami, A. Feizi, and R. Aghlmand. 2022. "Comparison of Results of Flood Hazard Zoning Using AHP and ANP Methods in GIS Environment: A Case Study in Ardabil Province, Iran." *Journal of Applied Research in Water and Wastewater* 9, no. 1: 1–7.

Darwish, K. 2023. "GIS-Based Multi-Criteria Decision Analysis for Flash Flood Hazard and Risk Assessment: A Case Study of the Eastern Minya Watershed, Egypt." *The 7th International Electronic Conference on Water Sciences*, vol. 87. https://doi.org/10.3390/ECWS-7-14315.

Dash, P., and J. Sar. 2020. "Identification and Validation of Potential Flood Hazard Area Using GIS-Based Multi-Criteria Analysis and Satellite Data-Derived Water Index." *Journal of Flood Risk Management* 13, no. 3. https://doi.org/10.1111/jfr3.12620.

Dehghani, T., A. Mohammadi, F. G. Sofloo, H. Ahmadpari, and T. N. Peykani. 2021. "Flood Risk Zoning by Combining Fuzzy AHP Approach and GIS (Case Study: Aligudarz-Azna Basin)." *International Journal of Pharmaceutical Research* 13, no. 1. https://doi.org/10.31838/ijpr/2021.13.01.810.

Desalegn, H., and A. Mulu. 2021. "Flood Vulnerability Assessment Using GIS at Fetam Watershed, Upper Abbay Basin, Ethiopia." *Heliyon* 7, no. 1: e05865. https://doi.org/10.1016/j.heliyon.2020.e05865.

Dozier, J. 1989. "Spectral Signature of Alpine Snow Cover From the Landsat Thematic Mapper." *Remote Sensing of Environment* 28: 9–22. https://doi.org/10.1016/0034-4257(89)90101-6.

Duan, C., J. Zhang, Y. Chen, et al. 2022. "Comprehensive Risk Assessment of Urban Waterlogging Disaster Based on MCDA-GIS Integration: The Case Study of Changchun, China." *Remote Sensing* 14, no. 13: 3101. https://doi.org/10.3390/rs14133101.

Ebodé, V. B., R. Onguéné, and J. J. Braun. 2024. "Flood Susceptibility Mapping in the Tongo Bassa Watershed Through GIS, Remote Sensing and Frequency Ratio Model." *Hydrology Research* 55, no. 4: 484–497. https://doi.org/10.2166/nh.2024.152.

Enomah, L. D., J. Downs, N. Mbaigoto, B. Fonda, and M. Umar. 2023. "Flood Risk Assessment in Limbe (Cameroon) Using a GIS Weighed Sum Method." *Environment, Development and Sustainability* 26. https://doi.org/10.1007/s10668-023-03836-3.

Eyeta, O. K., A. S. Alalade, and B. Momohjimoh. 2023. "Flood Vulnerability Assessment of Delta State Utilizing Remote Sensing and Geographic Information System (GIS)." *Journal of Energy Technology and Environment* 5, no. 4: 2023–2060. https://doi.org/10.5281/zenodo.10431948.

Faregh, W., and A. Benkhaled. 2021. "GIS-Based Multicriteria Approach for Flood Risk Assessment in Sigus City, East Algeria." *Arabian Journal of Geosciences* 14, no. 12: 1152. https://doi.org/10.1007/s12517-021-07314-w.

14679671, 2026, 1, Downloaded from https://onlinelibrary.wiley.com/doi/10.1111/tgis.70190 by Serdar Selim - Akdeniz University , Wiley Online Library on [08/02/2026]. See the Terms and Conditions (https://onlinelibrary.wiley.com/terms-and-conditions) on Wiley Online Library for rules of use; OA articles are governed by the applicable Creative Commons License

Farhadi, H., and M. Najafzadeh. 2021. "Flood Risk Mapping by Remote Sensing Data and Random Forest Technique." *Water* 13, no. 21: 3115. https://doi.org/10.3390/w13213115.

Fatah, K. K., Y. T. Mustafa, and I. O. Hassan. 2022. "Flood Susceptibility Mapping Using an Analytic Hierarchy Process Model Based on Remote Sensing and GIS Approaches in Akre District, Kurdistan Region, Iraq." *Iraqi Geological Journal* 55, no. 2C: 121–149. https://doi.org/10.46717/igj.55.2C.10ms-2022-08-23.

Fenglin, W., I. Ahmad, M. Zelenakova, et al. 2023. "Exploratory Regression Modeling for Flood Susceptibility Mapping in the GIS Environment." *Scientific Reports* 13, no. 1: 247. https://doi.org/10.1038/s41598-023-27447-0.

Gacu, J. G., C. E. F. Monjardin, D. B. Senoro, and F. J. Tan. 2022. "Flood Risk Assessment Using GIS-Based Analytical Hierarchy Process in the Municipality of Odiongan, Romblon, Philippines." *Applied Sciences* 12, no. 19: 9456. https://doi.org/10.3390/app12199456.

Gahalod, N. S. S., K. Rajeev, P. K. Pant, S. Binjola, R. L. Yadav, and R. L. Meena. 2024. "Spatial Assessment of Flood Vulnerability and Waterlogging Extent in Agricultural Lands Using RS-GIS and AHP Technique—A Case Study of Patan District Gujarat, India." *Environmental Monitoring and Assessment* 196, no. 4: 338. https://doi.org/10.1007/s10661-024-12482-9.

Gautam, P. K., and D. S. Singh. 2022. "Flood Hazard and Risk Assessment of Deoha River Basin, Central Ganga Plain, India: An GIS Approach." *Disaster Advances* 15, no. 10: 42–51. https://doi.org/10.25303/1510da042051.

Ghosh, A., U. Chatterjee, S. C. Pal, A. R. M. Towfiqul Islam, E. Alam, and M. K. Islam. 2023. "Flood Hazard Mapping Using GIS-Based Statistical Model in Vulnerable Riparian Regions of Sub-Tropical Environment." *Geocarto International* 38, no. 1. https://doi.org/10.1080/10106049.2023.2285355.

Ghute, B. B., and P. Sarma. 2023. "A GIS-Based Flood Risk Assessment and Mapping Using Morphometric Analysis in the Kayadhu River Basin, Maharashtra." In *River Conservation and Water Resource Management*, 77–93. Springer Nature Singapore. https://doi.org/10.1007/978-981-99-2605-3_5.

Girma, D. 2023. "Flood Vulnerability and Risk Assessment Using the Integration of Analytical Hierarchy Process (AHP), GIS, and Remote Sensing: A Case Study of Southern Oromia Region." *OPSearch: American Journal of Open Research* 2, no. 2: 128–144. https://doi.org/10.58811/opsearch.v2i2.30.

Gupta, L., and J. Dixit. 2022. "A GIS-Based Flood Risk Mapping of Assam, India, Using the MCDA-AHP Approach at the Regional and Administrative Level." *Geocarto International* 37, no. 26: 11867–11899. https://doi.org/10.1080/10106049.2022.2060329.

Gupta, L., and J. Dixit. 2023. "Assessment of Urban Flood Susceptibility and Role of Urban Green Space (UGS) on Flooding Susceptibility Using GIS-Based Probabilistic Models." *Environmental Monitoring and Assessment* 195, no. 12: 1518. https://doi.org/10.1007/s10661-023-12061-4.

Gurer, I., and H. Ozguler. 2004. "Turkey: Recent Flood Disasters in Northwestern Black Sea Region." In *WMO/GWP Associated Programme on Flood Management*, 1–20.

Hagos, Y. G., T. G. Andualem, M. Yibeltal, and M. A. Mengie. 2022. "Flood Hazard Assessment and Mapping Using GIS Integrated With Multi-Criteria Decision Analysis in Upper Awash River Basin, Ethiopia." *Applied Water Science* 12, no. 7: 148. https://doi.org/10.1007/s13201-022-01674-8.

Hall, D. K., G. A. Riggs, and V. V. Salomonson. 1995. "Development of Methods for Mapping Global Snow Cover Using Moderate Resolution Imaging Spectroradiometer Data." *Remote Sensing of Environment* 54, no. 2: 127–140.

Haltas, I., E. Yildirim, F. Oztas, and I. Demir. 2021. "A Comprehensive Flood Event Specification and Inventory: 1930–2020 Turkey Case Study." *International Journal of Disaster Risk Reduction* 56: 102086. https://doi.org/10.1016/j.ijdrr.2021.102086.

Hammami, S., L. Zouhri, D. Souissi, et al. 2019. "Application of the GIS Based Multi-Criteria Decision Analysis and Analytical Hierarchy Process (AHP) in the Flood Susceptibility Mapping (Tunisia)." *Arabian Journal of Geosciences* 12, no. 21: 653. https://doi.org/10.1007/s12517-019-4754-9.

Hassan, Z., and A. N. Kamarudzaman. 2022. "Development of Flood Hazard Index (FHI) of the Kelantan River Catchment Using Geographic Information System (GIS) Based Analytical Hierarchy Process (AHP)." *Pertanika Journal of Science and Technology* 31, no. 1: 203–215. https://doi.org/10.47836/pjst.31.1.13.

Heymann, Y. 1994. *CORINE Land Cover: Technical Guide*. Office for Official Publications Office of the European Communities.

Hoang, V. D., H. T. Tran, and T. T. Nguyen. 2020. "A GIS-Based Spatial Multi-Criteria Approach for Flash Flood Risk Assessment in the Ngan Sau-Ngan Pho Mountainous River Basin, North Central of Vietnam." *Environment and Natural Resources Journal* 18, no. 2: 110–123. https://doi.org/10.32526/ennrj.18.2.2020.11.

Hossain, M. K., and Q. Meng. 2020. "A Fine-Scale Spatial Analytics of the Assessment and Mapping of Buildings and Population at Different Risk Levels of Urban Flood." *Land Use Policy* 99: 104829. https://doi.org/10.1016/j.landusepol.2020.104829.

Hussain, M., M. Tayyab, K. Ullah, et al. 2023. "Development of a New Integrated Flood Resilience Model Using Machine Learning With GIS-Based Multi-Criteria Decision Analysis." *Urban Climate* 50: 101589. https://doi.org/10.1016/j.uclim.2023.101589.

Hussain, M., M. Tayyab, J. Zhang, et al. 2021. "GIS-Based Multi-Criteria Approach for Flood Vulnerability Assessment and Mapping in District Shangla: Khyber Pakhtunkhwa, Pakistan." *Sustainability* 13, no. 6: 3126. https://doi.org/10.3390/su13063126.

Ighile, E. H., H. Shirakawa, and H. Tanikawa. 2022. "Application of GIS and Machine Learning to Predict Flood Areas in Nigeria." *Sustainability* 14, no. 9: 5039. https://doi.org/10.3390/su14095039.

Indrayani, P., I. Djamaluddin, and Y. Cai. 2023. "Employing a Local Framework and GIS to Evaluate the Flood Risk Index Maps of Makassar City, Indonesia." *Arabian Journal of Geosciences* 16, no. 10: 568. https://doi.org/10.1007/s12517-023-11664-y.

Iroume, J. Y. A., R. Onguéné, F. Djanna Koffi, et al. 2022. "The 21st August 2020 Flood in Douala (Cameroon): A Major Urban Flood Investigated With 2D HEC-RAS Modeling." *Water* 14, no. 11. https://doi.org/10.3390/w14111768.

Isiaka, I. O., S. Gafar, S. A. Ajadi, I. Mukaila, K. O. Ndukwe, and S. O. Mustapha. 2023. "Flood Susceptibility Assessment of Lagos State, Nigeria Using Geographical Information System (GIS)-Based Frequency Ratio Model." *International Journal of Environment and Geoinformatics* 10, no. 1: 76–89. https://doi.org/10.30897/ijegeo.1181698.

Islam, M. M., K. Ujiie, R. Noguchi, and T. Ahamed. 2022. "Flash Flood-Induced Vulnerability and Need Assessment of Wetlands Using Remote Sensing, GIS, and Econometric Models." *Remote Sensing Applications: Society and Environment* 25: 100692. https://doi.org/10.1016/j.rsase.2021.100692.

Jagtap, A. A., D. K. Shedge, V. Degaonkar, and V. R. Chowdhary. 2023. "Flood Risk Area Identification of Pune District Using GIS Techniques." *9th International Conference on Advanced Computing and Communication Systems (ICACCS)*, 1326–1331. https://doi.org/10.1109/ICACCS57279.2023.10112874.

Karymbalis, E., M. Andreou, D.-V. Batzakis, K. Tsanakas, and S. Karalis. 2021. "Integration of GIS-Based Multicriteria Decision Analysis and Analytic Hierarchy Process for Flood-Hazard Assessment in the

14679671, 2026, 1, Downloaded from https://onlinelibrary.wiley.com/doi/10.1111/tgis.70190 by Serdar Selim - Akdeniz University , Wiley Online Library on [08/02/2026]. See the Terms and Conditions (https://onlinelibrary.wiley.com/terms-and-conditions) on Wiley Online Library for rules of use; OA articles are governed by the applicable Creative Commons License

Megalo Rema River Catchment (East Attica, Greece)." *Sustainability* 13, no. 18: 10232. https://doi.org/10.3390/su131810232.

Kaya, Y. Z., and F. Üneş. 2025. "Comparison of Three Different Satellite Data on 2D Flood Modeling Using HEC-RAS (5.0.7) Software and Investigating the Improvement Ability of the RAS Mapper Tool." *Journal of Flood Risk Management* 18, no. 1. https://doi.org/10.1111/jfr3.13046.

Khan, Z. A., and B. Jhamnani. 2024. "Development of Flood Susceptibility Map Using a GIS-Based AHP Approach: A Novel Case Study on Idukki District, India." *Journal of Spatial Science* 69, no. 2: 409–442. https://doi.org/10.1080/14498596.2023.2236051.

Khoirunisa, N., C.-Y. Ku, and C.-Y. Liu. 2021. "A GIS-Based Artificial Neural Network Model for Flood Susceptibility Assessment." *International Journal of Environmental Research and Public Health* 18, no. 3: 1072. https://doi.org/10.3390/ijerph18031072.

Kittipongvises, S., A. Phetrak, P. Rattanapun, K. Brundiers, J. L. Buizer, and R. Melnick. 2020. "AHP-GIS Analysis for Flood Hazard Assessment of the Communities Nearby the World Heritage Site on Ayutthaya Island, Thailand." *International Journal of Disaster Risk Reduction* 48: 101612. https://doi.org/10.1016/j.ijdrr.2020.101612.

Koç, G., and A. H. Thieken. 2018. "The Relevance of Flood Hazards and Impacts in Turkey: What Can Be Learned From Different Disaster Loss Databases?" *Natural Hazards* 91, no. 1: 375–408. https://doi.org/10.1007/s11069-017-3134-6.

Koem, C., and S. Tantanee. 2021. "Flash Flood Hazard Mapping Based on AHP With GIS and Satellite Information in Kampong Speu Province, Cambodia." *International Journal of Disaster Resilience in the Built Environment* 12, no. 5: 457–470. https://doi.org/10.1108/IJDRBE-09-2020-0099.

Kongmuang, C., S. Tantanee, and K. Seejata. 2020. "Urban Flood Hazard Map Using GIS of Muang Sukhothai District, Thailand." *Geographia Technica* 15, no. 1: 143–152. https://doi.org/10.21163/GT_2020.151.13.

Kourgialas, N. N., and G. P. Karatzas. 2016. "A Flood Risk Decision Making Approach for Mediterranean Tree Crops Using GIS; Climate Change Effects and Flood-Tolerant Species." *Environmental Science & Policy* 63: 132–142. https://doi.org/10.1016/j.envsci.2016.05.020.

Kumar, N., and R. Jha. 2023. "GIS-Based Flood Risk Mapping: The Case Study of Kosi River Basin, Bihar, India." *Engineering, Technology & Applied Science Research* 13, no. 1: 9830–9836. https://doi.org/10.48084/etasr.5377.

Lin, L., Z. Wu, and Q. Liang. 2019. "Urban Flood Susceptibility Analysis Using a GIS-Based Multi-Criteria Analysis Framework." *Natural Hazards* 97, no. 2: 455–475. https://doi.org/10.1007/s11069-019-03615-2.

Louis, R., Y. Zech, A. Joseph, N. Gonomy, and S. Soares-Frazao. 2024. "Flood Modeling of the June 2023 Flooding of Léogâne City by the Overflow of the Rouyonne River in Haiti." *Water* 16, no. 18: 2594. https://doi.org/10.3390/w16182594.

Loumi, K., and A. Redjem. 2021. "Integration of GIS and Hierarchical Multi-Criteria Analysis for Mapping Flood Vulnerability: The Case Study of M'sila, Algeria." *Engineering, Technology & Applied Science Research* 11, no. 4: 7381–7385. https://doi.org/10.48084/etasr.4266.

Luo, P., M. Luo, F. Li, et al. 2022. "Urban Flood Numerical Simulation: Research, Methods and Future Perspectives." *Environmental Modelling & Software* 156: 105478. https://doi.org/10.1016/j.envsoft.2022.105478.

M Amen, A. R., A. Mustafa, D. A. Kareem, et al. 2023. "Mapping of Flood-Prone Areas Utilizing GIS Techniques and Remote Sensing: A Case Study of Duhok, Kurdistan Region of Iraq." *Remote Sensing* 15, no. 4: 1102. https://doi.org/10.3390/rs15041102.

Mahmoody Vanolya, N., and M. Jelokhani-Niaraki. 2021. "The Use of Subjective–Objective Weights in GIS-Based Multi-Criteria Decision Analysis for Flood Hazard Assessment: A Case Study in Mazandaran, Iran." *GeoJournal* 86, no. 1: 379–398. https://doi.org/10.1007/s10708-019-10075-5.

Malik, S., S. C. Pal, A. Arabameri, et al. 2021. "GIS-Based Statistical Model for the Prediction of Flood Hazard Susceptibility." *Environment, Development and Sustainability* 23, no. 11: 16713–16743. https://doi.org/10.1007/s10668-021-01377-1.

Ministry of Culture and Tourism (MCT). 2024. *Accommodation Statistics for Business (Ministry) Certificated Facilities*. https://engelsiz.ktb.gov.tr/TR-201121/isletme-bakanlik-belgeli-tesis-konaklama-istatistikleri.html.

Mitra, R., P. Saha, and J. Das. 2022. "Assessment of the Performance of GIS-Based Analytical Hierarchical Process (AHP) Approach for Flood Modelling in Uttar Dinajpur District of West Bengal, India." *Geomatics, Natural Hazards and Risk* 13, no. 1: 2183–2226. https://doi.org/10.1080/19475705.2022.2112094.

Mohamd Hanan, N. A., M. A. Abas, A. N. Md Nor, et al. 2020. "A GIS-Based Flood Vulnerability Assessment in Pasir Mas, Kelantan." *IOP Conference Series: Earth and Environmental Science* 549, no. 1: 012004. https://doi.org/10.1088/1755-1315/549/1/012004.

Mohd Rasu, M. S., H. F. Suhandri, N. A. Khalifa, A. R. Abdul Rasam, and A. Hamid. 2023. "Evaluation of Flood Risk Map Development Through GIS-Based Multi-Criteria Decision Analysis in Maran District, Pahang—Malaysia." *International Journal of Geoinformatics* 19, no. 10: 1–16. https://doi.org/10.52939/ijg.v19i9.2873.

Msabi, M. M., and M. Makonyo. 2021. "Flood Susceptibility Mapping Using GIS and Multi-Criteria Decision Analysis: A Case of Dodoma Region, Central Tanzania." *Remote Sensing Applications: Society and Environment* 21: 100445. https://doi.org/10.1016/j.rsase.2020.100445.

Mukhtar, M. A., D. Shangguan, Y. Ding, et al. 2024. "Integrated Flood Risk Assessment in Hunza-Nagar, Pakistan: Unifying Big Climate Data Analytics and Multi-Criteria Decision-Making With GIS." *Frontiers in Environmental Science* 12. https://doi.org/10.3389/fenvs.2024.1337081.

Nadège, K. J., B. H. Akokponhoue, A. H. Bertrand, O. Vincent, and Y. Y. Muller. 2023. "Contribution of Multicriteria Analysis and GIS in the Discrimination of Flood Risk Areas on the Allada Plateau in Southern Benin." *International Journal of Innovation and Applied Studies* 38, no. 4: 906–924.

Narendr, A., S. Vinay, B. H. Aithal, and S. Das. 2022. "Multi-Dimensional Parametric Coastal Flood Risk Assessment at a Regional Scale Using GIS." *Environment, Development and Sustainability* 24, no. 7: 9569–9597. https://doi.org/10.1007/s10668-021-01839-6.

Nasr, A., M. Abdelkareem, and K. Moubark. 2022. "Integration of Remote Sensing and GIS for Mapping Flash Flood Hazards, Wadi Queih, Egypt." *SVU-International Journal of Agricultural Sciences* 4, no. 4: 197–206. https://doi.org/10.21608/svuijas.2023.186199.1264.

Noori, A., and H. Bonakdari. 2023. "A GIS-Based Fuzzy Hierarchical Modeling for Flood Susceptibility Mapping: A Case Study in Ontario, Eastern Canada." *ECWS-7* 2023: 62. https://doi.org/10.3390/ECWS-7-14242.

Nsangou, D., A. Kpoumié, Z. Mfonka, et al. 2022. "Urban Flood Susceptibility Modelling Using AHP and GIS Approach: Case of the Mfoundi Watershed at Yaoundé in the South-Cameroon Plateau." *Scientific African* 15: e01043. https://doi.org/10.1016/j.sciaf.2021.e01043.

Ogato, G. S., A. Bantider, K. Abebe, and D. Geneletti. 2020. "Geographic Information System (GIS)-based Multicriteria Analysis of Flooding Hazard and Risk in Ambo Town and Its Watershed, West Shoa Zone, Oromia Regional State, Ethiopia." *Journal of Hydrology: Regional Studies* 27: 100659. https://doi.org/10.1016/j.ejrh.2019.100659.

Olii, M. R., A. Olii, and R. Pakaya. 2021. "The Integrated Spatial Assessment of the Flood Hazard Using AHP-GIS: The Case Study of Gorontalo Regency." *Indonesian Journal of Geography* 53, no. 1: 126–135. https://doi.org/10.22146/ijg.59999.

14679671, 2026, 1, Downloaded from https://onlinelibrary.wiley.com/doi/10.1111/tgis.70190 by Serdar Selim - Akdeniz University , Wiley Online Library on [08/02/2026]. See the Terms and Conditions (https://onlinelibrary.wiley.com/terms-and-conditions) on Wiley Online Library for rules of use; OA articles are governed by the applicable Creative Commons License

Osman, S. A., and J. Das. 2023. "GIS-Based Flood Risk Assessment Using Multi-Criteria Decision Analysis of Shebelle River Basin in Southern Somalia." *SN Applied Sciences* 5, no. 5: 134. https://doi.org/10.1007/s42452-023-05360-5.

Özdemir, H., M. Baduna Koçyiğit, and D. Akay. 2023. "Flood Susceptibility Mapping With Ensemble Machine Learning: A Case of Eastern Mediterranean Basin, Türkiye." *Stochastic Environmental Research and Risk Assessment* 37, no. 11: 4273–4290. https://doi.org/10.1007/s00477-023-02507-z.

Parajuli, G., S. Neupane, S. Kunwar, R. Adhikari, and T. D. Acharya. 2023. "A GIS-Based Evacuation Route Planning in Flood-Susceptible Area of Siraha Municipality, Nepal." *ISPRS International Journal of Geo-Information* 12, no. 7: 286. https://doi.org/10.3390/ijgi12070286.

Pathan, A. I., and P. G. Agnihotri. 2021. "Application of New HEC-RAS Version 5 for 1D Hydrodynamic Flood Modeling With Special Reference Through Geospatial Techniques: A Case of River Purna at Navsari, Gujarat, India." *Modeling Earth Systems and Environment* 7, no. 2: 1133–1144. https://doi.org/10.1007/s40808-020-00961-0.

Pathan, A. I., P. Girish Agnihotri, S. Said, and D. Patel. 2022. "AHP and TOPSIS Based Flood Risk Assessment- a Case Study of the Navsari City, Gujarat, India." *Environmental Monitoring and Assessment* 194, no. 7: 509. https://doi.org/10.1007/s10661-022-10111-x.

Peker, İ. B., S. Gülbaz, V. Demir, O. Orhan, and N. Beden. 2024. "Integration of HEC-RAS and HEC-HMS With GIS in Flood Modeling and Flood Hazard Mapping." *Sustainability* 16, no. 3: 1226. https://doi.org/10.3390/su16031226.

Pham, B. T., M. Avand, S. Janizadeh, et al. 2020. "GIS Based Hybrid Computational Approaches for Flash Flood Susceptibility Assessment." *Water* 12, no. 3: 683. https://doi.org/10.3390/w12030683.

Pham, B. T., C. Luu, D. Van Dao, et al. 2021. "Flood Risk Assessment Using Deep Learning Integrated With Multi-Criteria Decision Analysis." *Knowledge-Based Systems* 219: 106899. https://doi.org/10.1016/j.knosys.2021.106899.

Pham, B. T., C. Luu, T. Van Phong, et al. 2021. "Flood Risk Assessment Using Hybrid Artificial Intelligence Models Integrated With Multi-Criteria Decision Analysis in Quang Nam Province, Vietnam." *Journal of Hydrology* 592: 125815. https://doi.org/10.1016/j.jhydrol.2020.125815.

Purwanto, A., R. Rustam, D. Andrasmoro, and E. Eviliyanto. 2022. "Flood Risk Mapping Using GIS and Multi-Criteria Analysis at Nanga Pinoh West Kalimantan Area." *Indonesian Journal of Geography* 54, no. 3: 463–470. https://doi.org/10.22146/ijg.69879.

Radwan, F., A. A. Alazba, and A. Mossad. 2019. "Flood Risk Assessment and Mapping Using AHP in Arid and Semiarid Regions." *Acta Geophysica* 67, no. 1: 215–229. https://doi.org/10.1007/s11600-018-0233-z.

Rahman, Z. U., W. Ullah, S. Bai, et al. 2023. "GIS-Based Flood Susceptibility Mapping Using Bivariate Statistical Model in Swat River Basin, Eastern Hindukush Region, Pakistan." *Frontiers in Environmental Science* 11. https://doi.org/10.3389/fenvs.2023.1178540.

Rai, K., N. Mishra, A. K. Sharma, S. Mishra, and P. P. Dahale. 2023. "Flood Risk Assessment Mapping of Nainital District Using GIS Tools." *2023 International Conference on Artificial Intelligence and Applications (ICAIA) Alliance Technology Conference (ATCON-1)*, 1–5. https://doi.org/10.1109/ICAIA57370.2023.10169591.

Rashwan, M., A. K. Mohamed, F. Alshehri, S. Almadani, M. Khattab, and L. Mohamed. 2023. "Flash Flood Hazard Assessment Along the Red Sea Coast Using Remote Sensing and GIS Techniques." *ISPRS International Journal of Geo-Information* 12, no. 11: 465. https://doi.org/10.3390/ijgi12110465.

Saaty, T. L. 1977. "A Scaling Method for Priorities in Hierarchical Structures." *Journal of Mathematical Psychology* 15, no. 3: 234–281. https://doi.org/10.1016/0022-2496(77)90033-5.

Saaty, T. L. 1980. "The Analytic Hierarchy Process (AHP)." *Journal of the Operational Research Society* 41, no. 11: 1073–1076. https://www.iasj.net/iasj/download/9c50d6dda6342d0f.

Saha, A. K., and S. Agrawal. 2020. "Mapping and Assessment of Flood Risk in Prayagraj District, India: A GIS and Remote Sensing Study." *Nanotechnology for Environmental Engineering* 5, no. 2: 11. https://doi.org/10.1007/s41204-020-00073-1.

Sakmongkoljit, K., N. Homtong, N. Surakotra, and N. Silaratana. 2021. "Multi-Criteria Flood Susceptibility Assessment Using Remote Sensing and GIS-Based Approaches in Chi River Basin, Thailand." *IOP Conference Series: Materials Science and Engineering* 1163, no. 1: 012025.

Samantaray, S., S. S. Das, A. Sahoo, and D. P. Satapathy. 2022. "Evaluating the Application of Metaheuristic Approaches for Flood Simulation Using GIS: A Case Study of Baitarani River Basin, India." *Materials Today: Proceedings* 61: 452–465. https://doi.org/10.1016/j.matpr.2021.11.561.

Sarchani, S., K. Seiradakis, P. Coulibaly, and I. Tsanis. 2020. "Flood Inundation Mapping in an Ungauged Basin." *Water* 12, no. 6: 1532. https://doi.org/10.3390/w12061532.

Sebastian, A., A. Juan, and P. B. Bedient. 2022. "Urban Flood Modeling: Perspectives, Challenges, and Opportunities." In *Coastal Flood Risk Reduction*, 47–60. Elsevier. https://doi.org/10.1016/B978-0-323-85251-7.00005-6.

Selim, S., E. Kahraman, C. Selim, et al. 2024. "Potential Flood Risk Scenario and Its Effects on Landscape Composition Using Hydraulic Modeling (HEC-RAS) in Boğaçay Sub-Basin/Türkiye." *Applied Sciences* 15, no. 1: 219. https://doi.org/10.3390/app15010219.

Selvam, R. A., and A. R. Antony Jebamalai. 2023. "Application of the Analytical Hierarchy Process (AHP) for Flood Susceptibility Mapping Using GIS Techniques in Thamirabarani River Basin, Srivaikundam Region, Southern India." *Natural Hazards* 118, no. 2: 1065–1083. https://doi.org/10.1007/s11069-023-06037-3.

Semaw, F., G. Zeleke, and A. Balew. 2022. "Evaluating Flood Risk Management Practices and Vulnerability Mapping in Alawuha Watershed (North Wollo Zone, Ethiopia) Using GIS and Remote Sensing." *Applied Geomatics* 14, no. 2: 347–367. https://doi.org/10.1007/s12518-022-00429-z.

Shadmehri Toosi, A., G. H. Calbimonte, H. Nouri, and S. Alaghmand. 2019. "River Basin-Scale Flood Hazard Assessment Using a Modified Multi-Criteria Decision Analysis Approach: A Case Study." *Journal of Hydrology* 574: 660–671. https://doi.org/10.1016/j.jhydrol.2019.04.072.

Shah, R. K., and R. K. Shah. 2023. "GIS-Based Flood Susceptibility Analysis Using Multi-Parametric Approach of Analytical Hierarchy Process in Majuli Island, Assam, India." *Sustainable Water Resources Management* 9, no. 5: 139. https://doi.org/10.1007/s40899-023-00924-0.

Shastrakar, U., P. Ghule, A. Jagtap, and V. Degaonkar. 2023. "Flood Risk Mapping Using GIS of Mumbai District, India." *2023 3rd International Conference on Innovative Sustainable Computational Technologies (CISCT)*, 1–6. https://doi.org/10.1109/CISCT57197.2023.10351332.

Souissi, D., A. Souie, A. Sebei, et al. 2022. "Flood Hazard Mapping and Assessment Using Fuzzy Analytic Hierarchy Process and GIS Techniques in Takelsa, Northeast Tunisia." *Arabian Journal of Geosciences* 15, no. 16: 1405. https://doi.org/10.1007/s12517-022-10541-4.

Souissi, D., L. Zouhri, S. Hammami, M. H. Msaddek, A. Zghibi, and M. Dlala. 2020. "GIS-Based MCDM – AHP Modeling for Flood Susceptibility Mapping of Arid Areas, Southeastern Tunisia." *Geocarto International* 35, no. 9: 991–1017. https://doi.org/10.1080/10106049.2019.1566405.

Stamellou, E., K. Kalogeropoulos, N. Stathopoulos, et al. 2021. "A GIS-Cellular Automata-Based Model for Coupling Urban Sprawl and Flood

14679671, 2026, 1, Downloaded from https://onlinelibrary.wiley.com/doi/10.1111/tgis.70190 by Serdar Selim - Akdeniz University , Wiley Online Library on [08/02/2026]. See the Terms and Conditions (https://onlinelibrary.wiley.com/terms-and-conditions) on Wiley Online Library for rules of use; OA articles are governed by the applicable Creative Commons License

Susceptibility Assessment." *Hydrology* 8, no. 4: 159. https://doi.org/10.3390/hydrology8040159.

Subraelu, P., A. Ahmed, A. A. Ebraheem, et al. 2023. "Risk Assessment and Mapping of Flash Flood Vulnerable Zones in Arid Region, Fujairah City, UAE-Using Remote Sensing and GIS-Based Analysis." *Water* 15, no. 15: 2802. https://doi.org/10.3390/w15152802.

Syakira, N., M. L. Tan, Z. Zulkafli, et al. 2023. "Assessment of Three GPM IMERG Products for GIS-Based Tropical Flood Hazard Mapping Using Analytical Hierarchy Process." *Water* 15, no. 12: 2195. https://doi.org/10.3390/w15122195.

Tayyab, M., J. Zhang, M. Hussain, et al. 2021. "GIS-Based Urban Flood Resilience Assessment Using Urban Flood Resilience Model: A Case Study of Peshawar City, Khyber Pakhtunkhwa, Pakistan." *Remote Sensing* 13, no. 10: 1864. https://doi.org/10.3390/rs13101864.

Trif, S., Ș. Bilașco, D. Petrea, S. Roșca, I. Fodorean, and I. Vescan. 2023. "Spatial Modeling Through GIS Analysis of Flood Risk and Related Financial Vulnerability: Case Study: Turcu River, Romania." *Applied Sciences* 13, no. 17. https://doi.org/10.3390/app13179869.

Tsai, Y.-L. S., A. Dietz, N. Oppelt, and C. Kuenzer. 2019. "Remote Sensing of Snow Cover Using Spaceborne SAR: A Review." *Remote Sensing* 11, no. 12: 1456. https://doi.org/10.3390/rs11121456.

Turkish State Meteorological Service (TSMS). 2024. *Official Statistics: General Statistical Data for Our Provinces*. Official Statistics: General Statistical Data for Our Provinces. https://www.mgm.gov.tr/veridegerlendirme/il-ve-ilceler-istatistik.aspx?k=A&m=ANTALYA.

Turkish Statistical Institute (TURKSTAT). 2024. *Address Based Population Registration System Results: Population of Municipalities, Villages and Quarters*. https://biruni.tuik.gov.tr/medas/?locale=en.

Ullah, K., and J. Zhang. 2020. "GIS-Based Flood Hazard Mapping Using Relative Frequency Ratio Method: A Case Study of Panjkora River Basin, Eastern Hindu Kush, Pakistan." *PLoS One* 15, no. 3: e0229153. https://doi.org/10.1371/journal.pone.0229153.

Vafa, H., and D. Z. Seker. 2023. "Flood Risk Susceptibility and Evaluation by AHP Technique in Denizli, Turkiye." *6th Intercontinental Geoinformation Days (IGD)* 612: 53–56.

Vajeethaveesin, T., T. Panboonyuen, S. Lawawironjwong, P. Srestasathiern, S. Jaiyen, and K. Jitkajornwanich. 2022. "A Performance Comparison Between GIS-Based and Neuron Network Methods for Flood Susceptibility Assessment in Ayutthaya Province." *Trends in Sciences* 19, no. 2: 2038. https://doi.org/10.48048/tis.2022.2038.

Vojtek, M., J. Vojteková, and Q. B. Pham. 2021. "GIS-Based Spatial and Multi-Criteria Assessment of Riverine Flood Potential: A Case Study of the Nitra River Basin, Slovakia." *ISPRS International Journal of Geo-Information* 10, no. 9: 578. https://doi.org/10.3390/ijgi10090578.

Waqas, H., L. Lu, A. Tariq, et al. 2021. "Flash Flood Susceptibility Assessment and Zonation Using an Integrating Analytic Hierarchy Process and Frequency Ratio Model for the Chitral District, Khyber Pakhtunkhwa, Pakistan." *Water* 13, no. 12: 1650. https://doi.org/10.3390/w13121650.

Xu, H. 2006. "Modification of Normalised Difference Water Index (NDWI) to Enhance Open Water Features in Remotely Sensed Imagery." *International Journal of Remote Sensing* 27, no. 14: 3025–3033. https://doi.org/10.1080/01431160600589179.

Yilmaz, O. S. 2022. "Flood Hazard Susceptibility Areas Mapping Using Analytical Hierarchical Process (AHP), Frequency Ratio (FR) and AHP-FR Ensemble Based on Geographic Information Systems (GIS): A Case Study for Kastamonu, Türkiye." *Acta Geophysica* 70, no. 6: 2747–2769. https://doi.org/10.1007/s11600-022-00882-9.

Yukseler, U., A. Toprak, E. Gul, and O. F. Dursun. 2023. "Flood Hazard Mapping Using M5 Tree Algorithms and Logistic Regression: A Case Study in East Black Sea Region." *Earth Science Informatics* 16, no. 3: 2033–2047. https://doi.org/10.1007/s12145-023-01013-8.

Zeng, Z., Y. Li, J. Lan, and A. R. Hamidi. 2021. "Utilizing User-Generated Content and GIS for Flood Susceptibility Modeling in Mountainous Areas: A Case Study of Jian City in China." *Sustainability* 13, no. 12: 6929. https://doi.org/10.3390/su13126929.

Zia, S., S. A. Shirazi, and M. Nasar-u-Minallah. 2021. "Vulnerability Assessment of Urban Floods in Lahore, Pakistan Using GIS Based Integrated Analytical Hierarchy Approach." *Proceedings of the Pakistan Academy of Sciences. A, Physical and Computational Sciences* 58, no. 1: 85–96. https://doi.org/10.53560/PPASA(58-1)604.

14679671, 2026, 1, Downloaded from https://onlinelibrary.wiley.com/doi/10.1111/tgis.70190 by Serdar Selim - Akdeniz University , Wiley Online Library on [08/02/2026]. See the Terms and Conditions (https://onlinelibrary.wiley.com/terms-and-conditions) on Wiley Online Library for rules of use; OA articles are governed by the applicable Creative Commons License

Appendix A

TABLE A1 | Factors and methods used in flood susceptibility mapping and flood risk assessment (literature review between 2019 and the first quarter of 2024).

No	References	Study area (Country)	Flood conditioning factors (mostly used)											Methods
			SL	LULC	EL	RF	DR	ST	DD	L/G	TWI	NDVI	HF	
1	Abdulalim and Damaty (2022)	Saudi Arabia	X		X					X	X	X		AHP
2	Ahmed et al. (2024)	India	X	X	X	X	X	X			X			AHP
3	Ajjur and Mogheir (2020)	Palestine	X	X	X		X							AHP
4	Akdeniz and Tuzcu (2023)	Turkey	X	X		X	X			X				AHP
5	Aksoy (2023)	Turkey	X	X		X	X	X						AHP
6	Al-Areeq et al. (2022)	Saudi Arabia	X	X	X	X	X	X		X	X		X	ML
7	Alarifi et al. (2022)	Saudi Arabia	X		X	X	X		X		X			AHP
8	Alharbi (2023)	Saudi Arabia	X		X	X		X	X					WOA
9	Ali et al. (2019)	India	X	X	X	X	X	X			X		X	AHP+
10	Ali et al. (2020)	Slovakia	X	X	X	X	X	X	X	X	X	X		MCDA + SM + ML
11	Alimi et al. (2023)	Nigeria	X	X	X		X		X		X	X		AHP
12	Allafta and Opp (2021)	Iraq-Iran	X	X	X	X	X	X	X	X				AHP
13	Aprillya and Chasanah (2022)	Indonesia	X			X		X						MCDA
14	Argaz et al. (2019)	Morocco	X	X	X	X	X			X				FREGLS
15	Arya and Singh (2021)	India	X	X		X		X	X	X				AHP
16	Aslan (2023)	Turkey	X	X	X	X	X	X	X	X	X	X		AHP
17	Aydin and Iban (2023)	Turkey	X	X	X	X	X			X	X	X	X	ML
18	Aydin and Sevgi Birincioğlu (2022)	Turkey	X	X	X	X	X	X		X				AHP
19	Ayenew and Kebede (2023)	Ethiopia	X	X			X	X	X					WOA
20	Bansal et al. (2022)	India	X	X	X		X		X					AHP
21	Bansal et al. (2023)	India	X	X	X	X	X	X	X	X	X			AHP
22	Baykal et al. (2023)	Turkey	X	X		X	X	X		X				AHP
23	Belazreg et al. (2024)	Algeria	X	X	X	X		X	X					AHP
24	Burayu et al. (2023)	Ethiopia	X	X	X	X	X	X	X		X			AHP
25	Cabrera and Lee (2019)	Philippines	X		X	X	X	X	X					AHP+

(Continues)

14679671, 2026, 1, Downloaded from https://onlinelibrary.wiley.com/doi/10.1111/tgis.70190 by Serdar Selim - Akdeniz University , Wiley Online Library on [08/02/2026]. See the Terms and Conditions (https://onlinelibrary.wiley.com/terms-and-conditions) on Wiley Online Library for rules of use; OA articles are governed by the applicable Creative Commons License

TABLE A1 | (Continued)

No	References	Study area (Country)	Flood conditioning factors (mostly used)											Methods
			SL	LULC	EL	RF	DR	ST	DD	L/G	TWI	NDVI	HF	
26	Cabrera and Lee (2020)	Philippines	X		X	X	X	X	X					AHP+
27	Cai et al. (2021)	China		X	X	X	X							AHP+
28	Chaulagain et al. (2023)	Nepal	X	X	X	X	X		X					AHP
29	Chen (2022)	China	X	X	X	X	X	X			X	X		AHP+
30	Chukwu et al. (2023)	Nigeria	X	X		X		X	X					AHP+
31	Chukwuma et al. (2021)	Nigeria	X	X	X	X	X	X	X					MCDA
32	Costache (2019)	Romania	X	X	X	X	X	X		X	X		X	ML+SM
33	Costache et al. (2022)	Romania	X	X	X	X	X	X		X	X		X	ML+SM
34	Daneshparvar et al. (2022)	Iran	X	X	X	X	X	X		X		X		AHP+
35	Darwish (2023)	Egypt	X	X	X	X	X	X	X	X				AHP
36	Dash and Sar (2020)	India	X	X	X				X	X				AHP
37	Dehghani et al. (2021)	Iran	X	X	X	X	X		X	X		X		AHP-Variant
38	Desalegn and Mulu (2021)	Ethiopia	X	X	X	X		X	X					AHP
39	Ebodé et al. (2024)	Cameroon	X	X	X		X	X	X				X	SM
40	Enomah et al. (2023)	Cameroon	X	X	X	X		X						AHP
41	Eyeta et al. (2023)	Nigeria	X	X	X			X	X					AHP
42	Faregh and Benkhaled (2021)	Algeria	X	X	X		X							AHP
43	Farhadi and Najafzadeh (2021)	Iran	X	X	X	X	X	X	X		X	X	X	ML
44	Fatah et al. (2022)	Iraq	X	X	X	X	X	X	X	X	X	X		AHP
45	Fenglin et al. (2023)	Ethiopia	X	X	X	X		X	X		X			SM
46	Gahalod et al. (2024)	India	X	X	X	X		X			X	X		AHP
47	Gautam and Singh (2022)	India	X	X		X		X	X					WOA
48	Girma (2023)	Ethiopia	X	X	X	X	X	X	X		X			AHP
49	Gupta and Dixit (2023)	India	X	X	X	X		X	X		X		X	SM
50	Hagos et al. (2022)	Ethiopia	X	X	X	X	X	X	X					AHP
51	Hammami et al. (2019)	Tunisia	X	X	X	X		X	X	X				AHP
52	Hassan and Kamarudzaman (2022)	Malaysia	X	X	X	X		X	X					AHP

(Continues)

14679671, 2026, 1, Downloaded from https://onlinelibrary.wiley.com/doi/10.1111/tgis.70190 by Serdar Selim - Akdeniz University , Wiley Online Library on [08/02/2026]. See the Terms and Conditions (https://onlinelibrary.wiley.com/terms-and-conditions) on Wiley Online Library for rules of use; OA articles are governed by the applicable Creative Commons License

TABLE A1 | (Continued)

No	References	Study area (Country)	Flood conditioning factors (mostly used)											Methods
			SL	LULC	EL	RF	DR	ST	DD	L/G	TWI	NDVI	HF	
53	Hossain and Meng (2020)	USA	X	X	X		X	X						AHP
54	Hussain et al. (2023)	Pakistan	X	X	X	X	X			X	X		X	AHP+
55	Ighile et al. (2022)	Nigeria	X	X	X	X	X	X			X		X	ML + SM
56	Isiaka et al. (2023)	Nigeria	X	X	X	X	X	X	X		X	X	X	SM
57	Islam et al. (2022)	Bangladesh	X	X	X	X	X		X				X	SM
58	Jagtap et al. (2023)	India	X	X		X	X	X						WOA
59	Karymbalis et al. (2021)	Greece	X	X	X		X			X				AHP
60	Khan and Jhamnani (2024)	India	X	X	X	X	X	X		X	X			AHP
61	Khoirunisa et al. (2021)	Taiwan	X		X	X			X		X	X	X	ML
62	Kittipongvises et al. (2020)	Thailand	X	X	X	X			X				X	AHP
63	Koem and Tantanee (2021)	Cambodia	X	X	X	X	X	X	X	X				AHP
64	Kongmuang et al. (2020)	Thailand	X	X	X	X	X	X	X				X	SM
65	Kumar and Jha (2023)	India	X	X	X	X	X		X					AHP
66	Loumi and Redjem (2021)	Algeria	X	X			X							AHP
67	M Amen et al. (2023)	Iraq	X	X	X	X	X	X		X	X			AHP
68	Mahmoody Vanolya and Jelokhani-Niaraki (2021)	Iran	X	X	X	X	X			X		X		AHP+
69	Malik et al. (2021)	India	X	X	X	X	X	X	X	X	X	X		AHP+
70	Mohamd Hanan et al. (2020)	Malaysia	X	X	X	X								WOA
71	Mohd Rasu et al. (2023)	Malaysia	X	X		X		X						AHP
72	Msabi and Makonyo (2021)	Tanzania	X	X	X			X	X	X				AHP
73	Mukhtar et al. (2024)	Pakistan	X	X	X	X	X	X			X			AHP
74	Nadège et al. (2023)	Benin	X	X		X		X	X					AHP
75	Noori and Bonakdari (2023)	Canada	X	X	X	X	X	X	X	X				AHP-Variant
76	Nsangou et al. (2022)	Cameroon	X	X	X	X	X		X	X	X			AHP
77	Ogato et al. (2020)	Ethiopia	X	X	X	X		X	X					AHP
78	Olii et al. (2021)	Indonesia	X	X	X	X	X	X						AHP

(Continues)

14679671, 2026, 1, Downloaded from https://onlinelibrary.wiley.com/doi/10.1111/tgis.70190 by Serdar Selim - Akdeniz University , Wiley Online Library on [08/02/2026]. See the Terms and Conditions (https://onlinelibrary.wiley.com/terms-and-conditions) on Wiley Online Library for rules of use; OA articles are governed by the applicable Creative Commons License

TABLE A1 | (Continued)

No	References	Study area (Country)	Flood conditioning factors (mostly used)											Methods
			SL	LULC	EL	RF	DR	ST	DD	L/G	TWI	NDVI	HF	
79	Osman and Das (2023)	Somalia	X		X	X	X	X	X	X				AHP
80	Özdemir et al. (2023)	Turkey	X		X	X	X		X		X		X	ML
81	Parajuli et al. (2023)	Nepal	X	X	X	X	X		X		X	X		AHP
82	Peker et al. (2024)	Turkey		X	X	X		X						HM
83	Pham et al. (2020)	Iran	X	X	X	X	X	X		X			X	ML
84	Pham, Luu, Van Dao, et al. (2021)	Vietnam	X	X	X	X	X		X	X	X		X	AHP+
85	Pham, Luu, Van Phong, et al. (2021)	Vietnam	X	X	X	X	X		X	X	X		X	AHP+
86	Purwanto et al. (2022)	Indonesia	X	X		X		X	X					WOA
87	Radwan et al. (2019)	Saudi Arabia	X	X		X			X					AHP
88	Rahman et al. (2023)	Pakistan	X	X	X	X			X		X	X		SM
89	Rai et al. (2023)	India	X		X				X					WOA
90	Saha and Agrawal (2020)	India	X	X	X				X		X			AHP
91	Sakmongkoljit et al. (2021)	Thailand		X	X		X	X	X	X				AHP
92	Samantaray et al. (2022)	India	X	X	X	X	X						X	ML
93	Selvam and Antony Jebamalai (2023)	India	X	X	X	X	X		X		X			AHP
94	Semaw et al. (2022)	Ethiopia	X		X	X	X	X	X					WOA
95	Shadmehri Toosi et al. (2019)	Iran	X	X	X	X	X	X						AHP+
96	Shah and Shah (2023)	India	X	X	X	X	X	X	X		X	X		AHP
97	Shastrakar et al. (2023)	India	X	X		X	X	X						WOA
98	Souissi et al. (2020)	Tunisia	X	X	X	X	X		X	X				AHP
99	Souissi et al. (2022)	Tunisia	X	X		X	X	X	X	X	X			AHP-Variant
100	Stamellou et al. (2021)	Greece	X	X	X	X	X			X				AHP+
101	Subraelu et al. (2023)	UAE	X	X	X	X		X	X	X				WOA
102	Syakira et al. (2023)	Malaysia	X	X	X	X	X	X	X	X				AHP
103	Ullah and Zhang (2020)	Pakistan	X	X	X	X			X		X	X	X	SM
104	Vafa and Seker (2023)	Turkey	X	X	X	X	X	X	X		X	X		AHP
105	Vajeethaveesin et al. (2022)	Thailand	X	X	X	X		X						AHP+

(Continues)

14679671, 2026, 1, Downloaded from https://onlinelibrary.wiley.com/doi/10.1111/tgis.70190 by Serdar Selim - Akdeniz Universitesi , Wiley Online Library on [08/02/2026]. See the Terms and Conditions (https://onlinelibrary.wiley.com/terms-and-conditions) on Wiley Online Library for rules of use; OA articles are governed by the applicable Creative Commons License

TABLE A1 | (Continued)

No	References	Study area (Country)	Flood conditioning factors (mostly used)											Methods
			SL	LULC	EL	RF	DR	ST	DD	L/G	TWI	NDVI	HF	
106	Vojtek et al. (2021)	Slovakia	X		X		X		X	X				AHP
107	Waqas et al. (2021)	Pakistan	X	X	X	X	X	X	X	X			X	AHP+
108	Yilmaz (2022)	Turkey	X	X	X	X	X			X	X	X	X	AHP+
109	Yukseler et al. (2023)	Turkey	X		X	X		X			X	X	X	ML + SM
110	Zeng et al. (2021)	China	X	X	X	X	X					X	X	ML
111	Zia et al. (2021)	Pakistan	X	X		X		X	X					AHP

No	References	Study area	Description	Methods
112–125	Bhuyan et al. (2024), Chakraborty and Mukhopadhyay (2019), Duan et al. (2022), Gacu et al. (2022), Ghosh et al. (2023), Gupta and Dixit (2022), Hoang et al. (2020) Hussain et al. (2021), Indrayani et al. (2023), Lin et al. (2019), Mitra et al. (2022), Narendr et al. (2022), Pathan et al. (2022), Tayyab et al. (2021)	India, India, China, Philippines, India, India, Vietnam, Pakistan, Indonesia, China, India, India, India, and Pakistan, respectively.	In these studies, in addition to or difference from the most frequently used parameters mentioned above; demographic (average age, gender ratio, literacy etc.), socioeconomic (job type, education etc.) and proximity to important facilities (e.g., health centers, schools etc.) were taken into account	AHP was mostly used in these studies as well
125–130	Abdelgawad et al. (2024), Abdo (2020), Ghute and Sarma (2023), Nasr et al. (2022), Rashwan et al. (2023)	Egypt, Syria, India, Egypt, and Egypt, respectively	In these studies, morphometric parameters were derived and used	MA

Abbreviations: AHP, analytic hierarchy process; DD, drainage density; DR, distance from river; EL, elevation; FREGLS, it takes its name from the initials of the factors taken into account (Kourgialas and Karatzas 2016); HF, historical floods; HM, hydrological methods; L/G, lithology/geology; LULC, land use/land cover; MA, morphological analysis; MCDA, multi-criteria decision analysis (other than AHP); ML, machine learning techniques; NDVI, normalized difference vegetation index; RF, rainfall; SL, slope; SM, statistical methods; ST, soil type/texture; TWI, topographic wetness index; WOA, weighted overlay analysis.

14679671, 2026, 1, Downloaded from https://onlinelibrary.wiley.com/doi/10.1111/tgis.70190 by Serdar Selim - Akdeniz University , Wiley Online Library on [08/02/2026]. See the Terms and Conditions (https://onlinelibrary.wiley.com/terms-and-conditions) on Wiley Online Library for rules of use; OA articles are governed by the applicable Creative Commons License

Appendix B

TABLE B1 | Interpolation method used for rainfall mapping and classification method for classifying factors (literature review between 2019 and the first quarter of 2024).

		Interpolation method used for rainfall mapping			Classification method used to classify factors		
No	**References**	**Inverse distance weighting (IDW)**	**Kriging**	**Other**	**Natural breaks (Jenks)**	**Equal interval**	**Other**
1	Ahmed et al. (2024)	X			X		
2	Akdeniz and Tuzcu (2023)			X			
3	Aksoy (2023)	X					
4	Al-Areeq et al. (2022)			X	X		
5	Alarifi et al. (2022)	X			X		
6	Ali et al. (2019)	X			X		
7	Ali et al. (2020)				X	X	X
8	Allafta and Opp (2021)		X				
9	Argaz et al. (2019)			X			
10	Arya and Singh (2021)	X					
11	Aslan (2023)	X					
12	Aydin and Iban (2023)				X		
13	Bansal et al. (2022)				X	X	
14	Bansal et al. (2023)	X			X	X	
15	Baykal et al. (2023)	X					
16	Belazreg et al. (2024)	X			X		
17	Bhuyan et al. (2024)	X					
18	Burayu et al. (2023)	X				X	
19	Girma (2023)	X				X	
20	Cabrera and Lee (2019)		X			X	
21	Cabrera and Lee (2020)		X				
22	Cai et al. (2021)		X				
23	Chakraborty and Mukhopadhyay (2019)	X					
24	Chaulagain et al. (2023)				X	X	
25	Chen (2022)	X			X		
26	Chukwu et al. (2023)	X			X		
27	Chukwuma et al. (2021)	X			X		
28	Costache (2019)	X			X		
29	Costache et al. (2022)			X	X		
30	Darwish (2023)	X					
31	Dash and Sar (2020)				X		
32	Desalegn and Mulu (2021)	X				X	
33	Duan et al. (2022)				X		
34	Enomah et al. (2023)				X		
35	Eyeta et al. (2023)				X		

(Continues)

14679671, 2026, 1, Downloaded from https://onlinelibrary.wiley.com/doi/10.1111/tgis.70190 by Serdar Selim - Akdeniz University , Wiley Online Library on [08/02/2026]. See the Terms and Conditions (https://onlinelibrary.wiley.com/terms-and-conditions) on Wiley Online Library for rules of use; OA articles are governed by the applicable Creative Commons License

TABLE B1 | (Continued)

No	References	Interpolation method used for rainfall mapping			Classification method used to classify factors		
		Inverse distance weighting (IDW)	Kriging	Other	Natural breaks (Jenks)	Equal interval	Other
36	Farhadi and Najafzadeh (2021)		X		X		
37	Fatah et al. (2022)		X		X		
38	Fenglin et al. (2023)			X	X		
39	Gacu et al. (2022)			X		X	
40	Gahalod et al. (2024)				X		
41	Gupta and Dixit (2022)	X			X		
42	Gupta and Dixit (2023)	X			X		
43	Hagos et al. (2022)	X					
44	Hammami et al. (2019)		X				
45	Hassan and Kamarudzaman (2022)		X				
46	Hossain and Meng (2020)				X		
47	Hussain et al. (2021)	X			X		
48	Hussain et al. (2023)				X		
49	Ighile et al. (2022)	X					X
50	Islam et al. (2022)	X					
51	Jagtap et al. (2023)	X					
52	Karymbalis et al. (2021)						X
53	Khan and Jhamnani (2024)	X			X		
54	Khoirunisa et al. (2021)		X		X		
55	Koem and Tantanee (2021)	X			X		
56	Kongmuang et al. (2020)				X		
57	Kumar and Jha (2023)	X			X		
58	Lin et al. (2019)		X		X		
59	M Amen et al. (2023)	X					
60	Malik et al. (2021)				X		
61	Mitra et al. (2022)				X	X	X
62	Mohamd Hanan et al. (2020)		X				
63	Mohd Rasu et al. (2023)	X					
64	Msabi and Makonyo (2021)					X	X
65	Mukhtar et al. (2024)	X					
66	Nadège et al. (2023)		X				
67	Narendr et al. (2022)						X
68	Noori and Bonakdari (2023)		X				
69	Nsangou et al. (2022)	X			X		
70	Ogato et al. (2020)	X				X	
71	Olii et al. (2021)	X					
72	Osman and Das (2023)	X			X		

(Continues)

14679671, 2026, 1, Downloaded from https://onlinelibrary.wiley.com/doi/10.1111/tgis.70190 by Serdar Selim - Akdeniz University , Wiley Online Library on [08/02/2026]. See the Terms and Conditions (https://onlinelibrary.wiley.com/terms-and-conditions) on Wiley Online Library for rules of use; OA articles are governed by the applicable Creative Commons License

TABLE B1 | (Continued)

No	References	Interpolation method used for rainfall mapping			Classification method used to classify factors		
		Inverse distance weighting (IDW)	Kriging	Other	Natural breaks (Jenks)	Equal interval	Other
73	Özdemir et al. (2023)	X					
74	Parajuli et al. (2023)	X			X		
75	Pathan et al. (2022)	X			X		
76	Pham et al. (2020)						X
77	Pham, Luu, Van Dao, et al. (2021)				X		
78	Pham, Luu, Van Phong, et al. (2021)				X		
79	Purwanto et al. (2022)	X					
80	Rahman et al. (2023)				X		
81	Sakmongkoljit et al. (2021)				X		
82	Selvam and Antony Jebamalai (2023)	X					
83	Semaw et al. (2022)	X					
84	Shadmehri Toosi et al. (2019)		X		X		
85	Shah and Shah (2023)	X			X		X
86	Souissi et al. (2020)		X				
87	Souissi et al. (2022)	X					X
88	Stamellou et al. (2021)			X			
89	Subraelu et al. (2023)				X		
90	Syakira et al. (2023)	X			X		X
91	Tayyab et al. (2021)				X		
92	Ullah and Zhang (2020)	X			X		
93	Vafa and Seker (2023)				X		
94	Vojtek et al. (2021)				X	X	X
95	Waqas et al. (2021)	X					
96	Yilmaz (2022)		X		X		
97	Yukseler et al. (2023)				X		
98	Zeng et al. (2021)				X		
99	Zia et al. (2021)	X				X	

14679671, 2026, 1, Downloaded from https://onlinelibrary.wiley.com/doi/10.1111/tgis.70190 by Serdar Selim - Akdeniz University , Wiley Online Library on [08/02/2026]. See the Terms and Conditions (https://onlinelibrary.wiley.com/terms-and-conditions) on Wiley Online Library for rules of use; OA articles are governed by the applicable Creative Commons License